Regularization of the fermion self-energy and the electromagnetic vertex in the Yukawa model within light-front dynamics

V. A. Karmanov,[1] J.-F. Mathiot,[2] and A. V. Smirnov[1]

[1]*Lebedev Physical Institute, Leninsky Prospekt 53, 119991 Moscow, Russia*

[2]*Laboratoire de Physique Corpusculaire, Université Blaise-Pascal, CNRS/IN2P3, 24 avenue des Landais, F-63177 Aubière Cedex, France*

(Received 11 December 2006; published 20 February 2007)

In light-front dynamics, the regularization of amplitudes by traditional cutoffs imposed on the transverse and longitudinal components of particle momenta corresponds to restricting the integration volume by a nonrotationally invariant domain. The result depends not only on the size of this domain (i.e., on the cutoff values), but also on its orientation determined by the position of the light-front plane. Explicitly covariant formulation of light-front dynamics allows us to parametrize the latter dependence in a very transparent form. If we decompose the regularized amplitude in terms of independent invariant amplitudes, extra (nonphysical) terms should appear, with spin structures which explicitly depend on the orientation of the light-front plane. The number of form factors, i.e., the coefficients of this decomposition, therefore also increases. The spin-$1/2$ fermion self-energy is determined by three scalar functions, instead of the two standard ones, while for the elastic electromagnetic vertex the number of form factors increases from two to five. In the present paper we calculate perturbatively all these form factors in the Yukawa model. Then we compare the results obtained in the two following ways: (i) by using the light-front dynamics graph technique rules directly; (ii) by integrating the corresponding Feynman amplitudes in terms of the light-front variables. For each of these methods, we use two types of regularization: the transverse and longitudinal cutoffs, and the Pauli-Villars regularization. In the latter case, the dependence of amplitudes on the light-front plane orientation vanishes completely provided enough Pauli-Villars subtractions are made.

DOI: 10.1103/PhysRevD.75.045012 PACS numbers: 11.10.−z, 11.15.Bt, 13.40.Gp

I. INTRODUCTION

Light-front dynamics (LFD) is extensively and successfully applied to hadron phenomenology, relativistic few-body systems, and field theory. For reviews of theoretical developments and applications see, e.g., Refs. [1,2]. In the LFD framework, nonperturbative approaches to field theory were developed in Refs. [3–5] and in Refs. [6–8]. In spite of some essential differences, these approaches proceed from the same starting point, namely, they approximate the state vector of the system by a truncated one. The problem is then solved without any decomposition in powers of the coupling constant. Doing that, one should carry out the renormalization procedure nonperturbatively. This is a nontrivial problem which is at the heart of ongoing intense research. However, before renormalization, one should regularize the amplitudes, both in the perturbative and nonperturbative frameworks. The explicit dependence of these amplitudes on the cutoffs is not unique. It is determined by the method of regularization.

It is of utmost importance to understand the origin and the implications of this dependence if one wants to address the question of nonperturbative renormalization. As we shall show in the present article, this is the only way to identify the structure of the counterterms needed to recover full rotationally invariant renormalized amplitudes in LFD. The question of the nonperturbative determination of the counterterms in truncated Fock space is discussed in Ref. [8].

The rules for calculating amplitudes can be derived directly, either by transforming the standard T-ordering of the S-matrix into the ordering along the light-front (LF) time (the LFD graph technique rules [1]), or from quantized field theory on the LF plane [2]. An alternative method consists in expressing well-defined Feynman amplitudes through the LF variables and integrating over the minus components of particle momenta [9,10]. Such an approach was applied to the derivation and study of the LF electromagnetic amplitudes [11,12] and to the analysis of different contributions to the electromagnetic current, resulting from the LF reduction of the Bethe-Salpeter formalism [13]. A study of electroweak transitions of the spin-1 mesons, based on using the LF plane of general orientation [1], was carried out in Refs. [14,15]. The comparison of perturbative amplitudes obtained from the LFD graph technique rules with those derived from the Feynman approach is, in general, not trivial, as shown in Ref. [16].

Concerning the regularization of amplitudes in LFD, at least two important features should be mentioned. First, if a given physical process is described by a set of LF diagrams, each partial LF amplitude usually diverges more strongly than the Feynman amplitude of the same process. The statement holds true regardless of the origin of the LF contributions: either from the rules of LFD, or from the Feynman amplitude. This increases the sensitivity of the result to the choice of the regularization procedure and may be a source of the so-called treacherous points [17].

Second, the LF variables (and, hence, the integration domain with the cutoffs imposed on it) explicitly depend on the LF plane orientation, which means the loss of rotational invariance. Because of this extra dependence, *standard* decompositions of such regularized LF amplitudes into invariant amplitudes are not valid. The total number of invariant amplitudes (and the number of form factors which are the coefficients in this decomposition) increases, as compared to the case when the rotational invariance is preserved. For example, the LF electromagnetic vertex (EMV) of a spin-$1/2$ particle is determined by five form factors rather than by two. In order to cancel the extra contributions (which depend on the LF plane orientation), one needs to introduce in the interaction Hamiltonian new specific counterterms.

This complication is especially dramatic in nonperturbative approaches, where the Fock space truncation is another source of the rotational symmetry violation. A given Feynman diagram may generate a few time-ordered ones with intermediate states containing a different number of particles. When they are truncated, the rotational invariance is lost even for invariant cutoffs. The interlacing of the two sources of the violation of rotational symmetry makes nonperturbative analysis of the counterterm structure extremely involved. One should therefore separate to a maximal extent the problems coming from the regularization procedure and from the Fock space truncation. That can be effectively done in the explicitly covariant formulation of LFD within the perturbative framework in a given order in the coupling constant.

In the present paper we study in detail this problem for the spin-$1/2$ fermion perturbative self-energy and the elastic EMV in the Yukawa model within the framework of explicitly covariant LFD [1]. The latter deals with the LF plane of general orientation $\omega \cdot x = \omega_0 t - \boldsymbol{\omega} \cdot \boldsymbol{x} = 0$, where ω is a four-vector with $\omega^2 = 0$. In the particular case $\omega = (1, 0, 0, -1)$ we recover the standard approach on the plane $t + z = 0$. Because of ω, which is transformed as a four-vector under rotations and Lorentz boosts, we can keep manifest rotational invariance throughout the calculations. Dependence of amplitudes on the LF plane orientation turns now in their dependence on the four-vector ω. The latter participates in the construction of the spin structures in which the regularized initial LF amplitude can be decomposed, on equal footing with the particle four-momenta. This generates extra (ω-dependent) spin structures with corresponding scalar coefficients (e.g., electromagnetic form factors). The number of the extra spin structures and their explicit forms are determined by general physical principles (more precisely, by the particle spins and the symmetries of the interaction), i.e., they are universal for any model and do not depend on particular features of dynamics; whereas, the dependence of the extra coefficients on particle four-momenta is determined by the model. This allows to separate general properties, related to LFD itself, from model-dependent effects.

We shall proceed in the following two ways, both for the self-energy and the EMV. In the first way, we calculate these quantities by the LFD graph technique rules, taking into account all necessary diagrams. In the second way, we start from the standard Feynman amplitudes and integrate them in terms of the LF variables. For both ways, we have to introduce cutoffs on the LF variables, and this fact already implies the contribution of extra (ω-dependent) structures and their corresponding form factors. The regularized self-energy and the EMV calculated by means of the LFD graph technique rules do not coincide in general with their counterparts obtained from the Feynman amplitudes. For the EMV case, the vertex found from the Feynman amplitude with the cutoffs imposed on the LF variables also differs from that calculated in a standard way, by the Wick rotation with a spherically symmetric cutoff or by the Pauli-Villars (PV) regularization. All these differences disappear when we deal with integrals which are finite from the very beginning (e.g., due to the PV regularization). They disappear also in the renormalized amplitudes, though renormalization procedures (counterterms, etc.) are drastically different for different regularization schemes.

Within covariant LFD, the perturbative QED self-energy and the EMV in the channel of the fermion-antifermion pair creation have been studied earlier [18]. The main subject was to extract the physical (ω-independent) contributions from the corresponding amplitudes and to renormalize this physical part only. The present analysis is devoted to a more detailed treatment of the self-energy and the EMV. We calculate both physical and nonphysical contributions in the two ways mentioned above and investigate the influence of the regularization procedure on the whole amplitudes and on their subsequent renormalization. The Yukawa model which we use reflects some features of QED but it is simpler from the technical point of view.

The paper is organized as follows. In Sec. II we briefly describe the LFD graph technique rules and apply them to calculate the fermion self-energy. We use two different regularization procedures, the transverse and longitudinal LF cutoffs or PV subtractions, either for the bosonic, or simultaneously for both bosonic and fermionic propagators. Then we calculate the fermion self-energy, starting from the manifestly invariant Feynman amplitude expressed through the LF variables and regularized in the same way as the LFD one. We compare the results obtained in both approaches and analyze how they are affected by the choice of regularization. In Sec. III we repeat analogous steps for the fermion EMV. For this purpose, we derive the LF interaction Hamiltonian which includes fermion-boson and fermion-photon interactions. We then construct the complete set of the LF diagrams which contribute to the EMV. We use again the noninvariant LF cutoffs and the invariant PV regularization. The LFD form factors are compared to those obtained in terms of the

Feynman amplitude with the same type of regularization. A general discussion of our results is presented in Sec. IV. Section V contains concluding remarks. The technical details of some derivations are given in the Appendices.

II. THE FERMION SELF-ENERGY

The fermion self-energy is the simplest example of how an extra spin structure is generated by rotationally noninvariant cutoffs in LFD. To make the situation more transparent, we will calculate the self-energy independently in the two following ways: (i) by applying the covariant LFD graph technique rules; (ii) by using the four-dimensional Feynman approach. In each case we consider two different types of regularization of divergent integrals: either the traditional rotationally noninvariant cutoffs or the invariant PV regularization. We then renormalize the amplitudes and compare the results obtained within these two methods.

A. Calculation in light-front dynamics

1. Light-front diagrams and their amplitudes

We calculate in this section the fermion self-energy in the second order of perturbation theory, using the graph technique rules of explicitly covariant LFD [1,7,19]. We do it in detail in order to explain the rules on a concrete example.

The self-energy $\Sigma(p)$ is determined by the sum of the two diagrams shown in Fig. 1,

$$\Sigma(p) = \Sigma_{2b}(p) + \Sigma_{fc}(p). \tag{1}$$

They correspond to the two-body contribution and the fermion contact term, respectively. Analytical expressions for the corresponding amplitudes read

$$\Sigma_{2b}(p) = -\frac{g^2}{(2\pi)^3}\int \theta(\omega\cdot k)\delta(k^2-\mu^2)d^4k(\not{q}+m) \times \theta(\omega\cdot q)\delta(q^2-m^2)d^4q\,\delta^{(4)}(p+\omega\tau-k-q) \times \frac{d\tau}{\tau - i0}, \tag{2a}$$

$$\Sigma_{fc}(p) = \frac{g^2}{(2\pi)^3}\int \frac{\not{\omega}}{2\omega\cdot(p-k)}\theta(\omega\cdot k)\delta(k^2-\mu^2)d^4k, \tag{2b}$$

where g is the coupling constant of the fermion-boson interaction, m and μ are the fermion and boson masses, respectively. In the covariant LFD graph technique, all the four-momenta are on the corresponding mass shells. This is due to the fact that the propagators are proportional to delta functions: $\theta(\omega\cdot k)\delta(k^2-\mu^2)$ is the boson propagator, $(\not{q}+m)\theta(\omega\cdot q)\delta(q^2-m^2)$ is the fermion one. Each theta function $\theta(\omega\cdot l)$ selects only one value of $l_0 = \sqrt{\boldsymbol{l} + m_l^2 2}$, of the two possible ones allowed by the corresponding delta function $\delta(l^2 - m_l^2)$. There is no conservation law for the components of particle four-momenta in the direction of ω (or for the minus components, in the standard version of LFD). The conservation is restored by the spurion four-momentum $\omega\tau$ which enters the delta function $\delta^{(4)}(p+\omega\tau-k-q)$. The factor $1/(\tau - i0)$ is the spurion propagator and the τ-integration is performed in infinite limits. To avoid misunderstanding, we emphasize that spurions are not true particles and do not affect particle counting. They serve as a convenient way to describe the departure of intermediate particles off the energy shell. The term "spurion" itself is used for shorter wording only. For this reason, the intermediate state in the self-energy (2a) contains one fermion and one scalar boson only. The self-energy is supposed to be off-energy-shell, i.e., $\tau_1 \neq 0$.

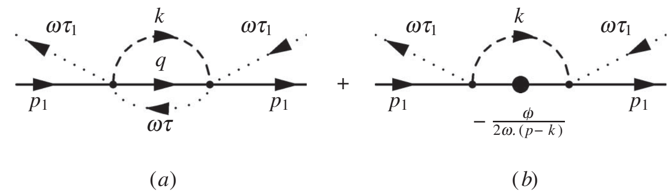

FIG. 1. Two contributions to the LFD fermion self-energy $-\Sigma(p)$: the two-body intermediate state (a) and the contact term (b). The solid, dashed, and dotted lines represent, respectively, the fermion, the boson, and the spurion. Here $p = p_1 - \omega\tau_1$, where $\omega\tau_1$ is the four-momentum attached to the initial (or final) spurion line. See text for the explanation.

Integrating by means of the delta functions over d^4q, $d\tau$, and dk_0, we get

$$\Sigma_{2b}(p) = -\frac{g^2}{(2\pi)^3}\int \frac{(\not{p}-\not{k}+\not{\omega}\tau+m)\theta[\omega\cdot(p-k)]}{2\omega\cdot(p-k)\tau}\frac{d^3k}{2\varepsilon_{\mathbf{k}}}, \tag{3a}$$

$$\Sigma_{fc}(p) = \frac{g^2\not{\omega}}{(2\pi)^3}\int \frac{1}{2\omega\cdot(p-k)}\frac{d^3k}{2\varepsilon_{\mathbf{k}}}, \tag{3b}$$

where $\varepsilon_{\mathbf{k}} \equiv k_0 = \sqrt{\mathbf{k}^2+\mu^2}$ and

$$\tau = \frac{m^2-(p-k)^2}{2\omega\cdot(p-k)}. \tag{4}$$

Let us go over to the LF variables. First, we denote $x = (\omega\cdot k)/(\omega\cdot p)$ (equivalent to k^+/p^+ in standard noncovariant LFD on the surface $t+z=0$). We then split the three-vector $\mathbf{k}$ into two parts: $\mathbf{k} = \mathbf{k}_\perp + \mathbf{k}_\parallel$, which are, respectively, perpendicular and parallel to the three-vector $\boldsymbol{\omega}$. Since $\Sigma(p)$ is an analytic function of p^2, we may calculate it for $p^2 > 0$, while its values for $p^2 \leq 0$ are obtained by the analytical continuation. If $p^2 > 0$, we may perform our calculation in the reference frame where $\mathbf{p} = \mathbf{0}$. Using the kinematical relations from Appendix A, one can rewrite Eqs. (3) as

$$\Sigma_{2b}(p) = -\frac{g^2}{16\pi^3}\int d^2k_\perp \int_0^1 \frac{(\not p - \not k + m)dx}{\mathbf{k}_\perp^2 + m^2x - p^2x(1-x) + \mu^2(1-x)} - \frac{g^2\not\omega}{32\pi^3(\omega\cdot p)}\int d^2k_\perp \int_0^1 \frac{dx}{x(1-x)}, \quad (5a)$$

$$\Sigma_{fc}(p) = \frac{g^2\not\omega}{32\pi^3(\omega\cdot p)}\int d^2k_\perp \int_0^{+\infty} \frac{dx}{x(1-x)}. \quad (5b)$$

Both $\Sigma_{2b}(p)$ and $\Sigma_{fc}(p)$ are expressed through integrals which diverge logarithmically in x and quadratically in $|\mathbf{k}_\perp|$. Possible regularization procedures are discussed below.

Following Ref. [7], we will use the matrix representation

$$\Sigma_{2b}(p) = g^2\left[\mathcal{A}(p^2) + \mathcal{B}(p^2)\frac{\not p}{m} + \mathcal{C}(p^2)\frac{m\not\omega}{\omega\cdot p}\right], \quad (6a)$$

$$\Sigma_{fc}(p) = g^2 C_{fc}\frac{m\not\omega}{\omega\cdot p}, \quad (6b)$$

where the coefficients $\mathcal{A}$, $\mathcal{B}$, and $\mathcal{C}$ are scalar functions which depend on p^2 only. They are independent of ω. The coefficient C_{fc} is a constant. The self-energy is thus obtained by summing up Eqs. (6):

$$\Sigma(p) = g^2\left\{\mathcal{A}(p^2) + \mathcal{B}(p^2)\frac{\not p}{m} + [\mathcal{C}(p^2) + C_{fc}]\frac{m\not\omega}{\omega\cdot p}\right\}. \quad (7)$$

Note that in expression (7) an additional spin structure proportional to $\not\omega$ appears, as compared to the standard four-dimensional Feynman approach.

2. Regularization with rotationally noninvariant cutoffs

In order to regularize the integrals over $d^2k_\perp$, we introduce a cutoff $\Lambda_\perp$, so that $\mathbf{k}_\perp^2 < \Lambda_\perp^2$. Since some integrals over dx diverge logarithmically at $x = 0$ and/or $x = 1$, we also introduce (where it is needed) an infinitesimal positive cutoff ϵ, assuming that x may belong to the intervals $\epsilon < x < 1-\epsilon$ and $1+\epsilon < x < +\infty$. The corresponding analytical expressions for the functions $\mathcal{A}(p^2)$, $\mathcal{B}(p^2)$, $\mathcal{C}(p^2)$, and C_{fc} were found in Ref [7]:

$$\mathcal{A}(p^2) = -\frac{m}{16\pi^2}\int_0^{\Lambda_\perp^2} d\mathbf{k}_\perp^2 \int_0^1 dx \frac{1}{\mathbf{k}_\perp^2 + m^2x - p^2x(1-x) + \mu^2(1-x)}, \quad (8a)$$

$$\mathcal{B}(p^2) = -\frac{m}{16\pi^2}\int_0^{\Lambda_\perp^2} d\mathbf{k}_\perp^2 \int_0^1 dx \frac{1-x}{\mathbf{k}_\perp^2 + m^2x - p^2x(1-x) + \mu^2(1-x)}, \quad (8b)$$

$$\mathcal{C}(p^2) = -\frac{1}{32\pi^2 m}\int_0^{\Lambda_\perp^2} d\mathbf{k}_\perp^2 \int_0^{1-\epsilon} dx \frac{k_\perp^2 + m^2 - p^2(1-x)^2}{(1-x)[\mathbf{k}_\perp^2 + m^2x - p^2x(1-x) + \mu^2(1-x)]}, \quad (8c)$$

$$C_{fc} = \frac{1}{32\pi^2 m}\int_0^{\Lambda_\perp^2} d\mathbf{k}_\perp^2\left[\int_\epsilon^{1-\epsilon}\frac{dx}{x(1-x)} + \int_{1+\epsilon}^{+\infty}\frac{dx}{x(1-x)}\right]. \quad (8d)$$

We imply in the following that $\Lambda_\perp^2 \gg \max\{|p^2|, m^2, \mu^2\}$ and $\epsilon \ll 1$. The dependence of physical results on the cutoffs is eliminated by taking the limits $\Lambda_\perp \to \infty$, $\epsilon \to 0$. Retaining in Eqs. (8) all terms which do not vanish in these limits, we get

$$\mathcal{A}(p^2) = -\frac{m}{8\pi^2}\log\frac{\Lambda_\perp}{m} + \frac{m}{16\pi^2}\int_0^1 dx \log\left[\frac{m^2x - p^2x(1-x) + \mu^2(1-x)}{m^2}\right], \quad (9a)$$

$$\mathcal{B}(p^2) = -\frac{m}{16\pi^2}\log\frac{\Lambda_\perp}{m} + \frac{m}{16\pi^2}\int_0^1 dx(1-x)\log\left[\frac{m^2x - p^2x(1-x) + \mu^2(1-x)}{m^2}\right], \quad (9b)$$

$$\mathcal{C}(p^2) = -\frac{\Lambda_\perp^2}{32\pi^2 m}\log\frac{1}{\epsilon} - \frac{m^2-\mu^2}{16\pi^2 m}\log\frac{\Lambda_\perp}{m} - \frac{1}{32\pi^2 m}\left(m^2 - \mu^2 - 2\mu^2\log\frac{m}{\mu}\right), \quad (9c)$$

$$C_{fc} = \frac{\Lambda_\perp^2}{32\pi^2 m}\log\frac{1}{\epsilon}. \quad (9d)$$

We have not integrated over dx in Eqs. (9a) and (9b) because the results of the integrations are rather long. It is interesting to note that $\mathcal{C}(p^2)$ does not depend on p^2. Because of this, we will denote in the following $\mathcal{C}(p^2) \equiv C =$ const and, for shortness, $\tilde{C} \equiv C + C_{fc}$.

Each of the two quantities, C and C_{fc}, diverges like $\Lambda_\perp^2\log(1/\epsilon)$. The strongest divergencies cancel in the sum $\tilde{C} = C + C_{fc}$, but the latter differs from zero and, moreover, has no finite limit when $\Lambda_\perp \to \infty$:

$$\tilde{C} = -\frac{m^2-\mu^2}{16\pi^2 m}\log\frac{\Lambda_\perp}{m} - \frac{1}{32\pi^2 m}\left(m^2-\mu^2-2\mu^2\log\frac{m}{\mu}\right). \tag{10}$$

Since the two diagrams shown in Fig. 1 exhaust the full set of the second-order diagrams which contribute to the fermion self-energy, we might expect the disappearance of every ω-dependent contribution from the amplitude. As far as this does not take place, the only source of the ω-dependence is the use of the rotationally noninvariant cutoffs for the LF variables $\mathbf{k}_\perp^2$ and x. Indeed, if we write these variables in the explicitly covariant form

$$\mathbf{k}_\perp^2 = 2\frac{(\omega\cdot k)(k\cdot p)}{\omega\cdot p} - p^2\left(\frac{\omega\cdot k}{\omega\cdot p}\right)^2 - \mu^2, \qquad x = \frac{\omega\cdot k}{\omega\cdot p},$$

it becomes evident that both of them depend on ω. Introducing the cutoffs $\Lambda_\perp^2$ and ϵ, we restrict an ω-dependent integration domain, which inevitably brings ω-dependence into the regularized quantities. We will demonstrate this feature in more detail in Sec. IV by using a very simple and transparent example. Note that, without adding new, ω-dependent, counterterms in the interaction Hamiltonian, this dependence is not killed by the standard renormalization. The renormalization recipe must be therefore modified [7].

3. Invariant Pauli-Villars regularization

As we learned above, the source of the appearance of the extra (ω-dependent) term in the regularized fermion self-energy is the ω-dependence of the integration domain. A standard way free from this demerit is the use of the PV regularization, since in that case the cutoffs have no more relation to ω. In the language of LFD, the PV regularization consists in changing the propagators as

$$\theta(\omega\cdot k)\delta(k^2-\mu^2) \to \theta(\omega\cdot k)[\delta(k^2-\mu^2) - \delta(k^2-\mu_1^2)]$$

for scalar bosons, and

$$(\not{q}+m)\theta(\omega\cdot q)\delta(q^2-m^2) \to \theta(\omega\cdot q)[(\not{q}+m)\delta(q^2-m^2) - (\not{q}+m_1)\delta(q^2-m_1^2)]$$

for fermions. This procedure is equivalent to introducing additional particles (one PV fermion with the mass m_1 and one PV boson with the mass μ_1), whose wave functions have negative norms. If needed, more subtractions can be done until all integrals become convergent. After the calculation of the integrals and the renormalization, the limits $\mu_1 \to \infty$ and $m_1 \to \infty$ should be taken. In the case of the fermion self-energy, we may regularize either the boson propagator only, or the fermion one, or both simultaneously. Hereafter we will supply PV-regularized quantities with the superscript "PV, b" (when only the bosonic propagator is modified) or "PV, $b+f$" (when both bosonic and fermionic propagators are modified).

Let us now calculate the PV-regularized coefficients $\mathcal{A}(p^2)$, $\mathcal{B}(p^2)$, and $\tilde{C}$. We can start from the expressions (9), in spite of their dependence on the "old" cutoffs $\Lambda_\perp$ and ϵ. Indeed, the integrals in Eqs. (5) become regular, provided enough PV subtractions have been made. If so, they have definite limits at $\Lambda_\perp \to \infty$ and $\epsilon \to 0$.

The integrals for $\mathcal{A}(p^2)$ and $\mathcal{B}(p^2)$ become convergent after the regularization by a PV boson only:

$$\mathcal{A}^{\mathrm{PV},b}(p^2) = \mathcal{A}(p^2,m,\mu) - \mathcal{A}(p^2,m,\mu_1) = \frac{m}{16\pi^2}\int_0^1 dx \log\left[\frac{m^2x - p^2x(1-x) + \mu^2(1-x)}{m^2x - p^2x(1-x) + \mu_1^2(1-x)}\right], \tag{11a}$$

$$\mathcal{B}^{\mathrm{PV},b}(p^2) = \mathcal{B}(p^2,m,\mu) - \mathcal{B}(p^2,m,\mu_1) = \frac{m}{16\pi^2}\int_0^1 dx(1-x) \log\left[\frac{m^2x - p^2x(1-x) + \mu^2(1-x)}{m^2x - p^2x(1-x) + \mu_1^2(1-x)}\right]. \tag{11b}$$

The situation differs drastically for the coefficient $\tilde{C}$. After the bosonic PV regularization we get

$$\tilde{C}^{\mathrm{PV},b} = \frac{1}{32\pi^2 m}\left[(\mu^2-\mu_1^2)\left(1+2\log\frac{\Lambda_\perp}{m}\right) + 2\mu^2\log\frac{m}{\mu} - 2\mu_1^2\log\frac{m}{\mu 1}\right]. \tag{12}$$

Since the result is still divergent for $\Lambda_\perp \to \infty$, this regularization is not enough. The additional fermionic PV regularization requires some care because $\tilde{C}$ is a coefficient at the spin structure $m\not{\omega}/(\omega\cdot p)$ which itself depends on m. Hence, one should regularize the quantity $m\tilde{C}$:

$$(m\tilde{C})^{\mathrm{PV},b+f} = m\tilde{C}(m,\mu) - m\tilde{C}(m,\mu_1) - m_1\tilde{C}(m_1,\mu) + m_1\tilde{C}(m_1,\mu_1) = 0. \tag{13}$$

We see that after the double PV regularization the extra structure in Eq. (7), proportional to $\not{\omega}$, disappears, as it should. Note that Eq. (13) holds for arbitrary (i.e., not necessary infinite) PV masses m_1 and μ_1.

4. Renormalization procedure

The renormalized self-energy is obtained by using the standard procedure:

$$\Sigma_{\mathrm{ren}}^{\mathrm{PV},b+f}(p) = \Sigma^{\mathrm{PV},b+f}(p) - c_1 - c_2(\not{p}-m), \tag{14}$$

where

$$c_1 = \frac{\bar{u}(p)\Sigma^{\mathrm{PV},b+f}(p)u(p)}{2m}\bigg|_{p^2=m^2}, \tag{15a}$$

$$c_2 = \frac{1}{2m}\left\{\bar{u}(p)\frac{\partial\Sigma^{\mathrm{PV},b+f}(p)}{\partial \not{p}}u(p)\right\}_{p^2=m^2}. \tag{15b}$$

Finally,

$$\Sigma^{\mathrm{PV},b+f}_{\mathrm{ren}}(p) = g^2\left[\mathcal{A}_{\mathrm{ren}}(p^2) + \mathcal{B}_{\mathrm{ren}}(p^2)\frac{\not{p}}{m}\right], \tag{16}$$

with

$$\mathcal{A}_{\mathrm{ren}}(p^2) = \mathcal{A}(p^2) - \mathcal{A}(m^2) + 2m^2[\mathcal{A}'(m^2) + \mathcal{B}'(m^2)], \tag{17a}$$

$$\mathcal{B}_{\mathrm{ren}}(p^2) = \mathcal{B}(p^2) - \mathcal{B}(m^2) - 2m^2[\mathcal{A}'(m^2) + \mathcal{B}'(m^2)]. \tag{17b}$$

In order to calculate $\mathcal{A}_{\mathrm{ren}}(p^2)$ and $\mathcal{B}_{\mathrm{ren}}(p^2)$ we can use the initial functions $\mathcal{A}(p^2)$ and $\mathcal{B}(p^2)$ regularized either by the noninvariant cutoffs, Eqs. (9a) and (9b), or by means of the PV regularization, Eqs. (11). Any choice leads to the same result:

$$\mathcal{A}_{\mathrm{ren}}(p^2) = \frac{m}{16\pi^2}\int_0^1 dx[\phi_1(x) - \phi_2(x)], \tag{18a}$$

$$\mathcal{B}_{\mathrm{ren}}(p^2) = \frac{m}{16\pi^2}\int_0^1 dx(1-x)[\phi_1(x) + \phi_2(x)], \tag{18b}$$

where

$$\phi_1(x) = \log\left[\frac{m^2x - p^2x(1-x) + \mu^2(1-x)}{m^2x^2 + \mu^2(1-x)}\right],$$

$$\phi_2(x) = \frac{2m^2x(2-3x+x^2)}{m^2x^2 + \mu^2(1-x)}.$$

The remaining integrations over dx in Eqs. (18) are simple but lengthy.

B. Calculation in the four-dimensional Feynman approach

1. Regularization with rotationally noninvariant cutoffs

We showed above that the regularized fermion self-energy calculated within LFD with the traditional transverse ($\Lambda_\perp$) and longitudinal (ϵ) cutoffs contains an extra spin structure depending on ω. In order to understand the reasons of this behavior, we calculate here the self-energy in another way, following Ref. [9]. We start from the standard four-dimensional Feynman expression

$$\Sigma_F(p) = \frac{ig^2}{(2\pi)^4} \times \int d^4k \frac{\not{p} - \not{k} + m}{[k^2 - \mu^2 + i0][(p-k)^2 - m^2 + i0]}, \tag{19}$$

but perform the integrations in terms of the LF variables, with the corresponding cutoffs. For this purpose, we introduce the minus, plus, and transverse components of the four-momentum k:

$$k_- = k_0 - k_z, \qquad k_+ = k_0 + k_z, \qquad \mathbf{k}_\perp = (k_x, k_y),$$

and analogously for p. As in Sec. II A 1, we take, for convenience, the reference frame where $\mathbf{p} = \mathbf{0}$. In this frame $p_- = p^2/p_+$. Denoting $k_+ = xp_+$, we get

$$\Sigma_F(p) = \frac{ig^2p_+}{32\pi^4}\int d^2k_\perp \int_{-\infty}^{+\infty} dx \int_{-\infty}^{+\infty} dk_- \times \frac{1}{[k_-p_+x - \mathbf{k}_\perp^2 - \mu^2 + i0]} \times \frac{(\not{p} - \not{k} + m)}{[(p_- - k_-)p_+(1-x) - \mathbf{k}_\perp^2 - m^2 + i0]} \tag{20}$$

with

$$\not{k} = \frac{1}{2}\gamma_+k_- + \frac{x}{2}\gamma_-p_+ - \boldsymbol{\gamma}_\perp\cdot\mathbf{k}_\perp.$$

The integral over dk_- is calculated by using the principal value prescription:

$$\int_{-\infty}^{+\infty} dk_-(\cdots) = \lim_{L\to\infty}\int_{-L}^{L} dk_-(\cdots). \tag{21}$$

This integral is well defined unless $x = 0$ or $x = 1$. If $x = 0$ or $x = 1$, the integral (21) diverges on the upper and lower limits. So, the infinitesimal integration domains near the points $x = 0$ and $x = 1$ (the so-called zero modes) require special consideration. We introduce a cutoff ϵ in the variable x and represent $\Sigma(p)$ as a sum

$$\Sigma_F(p) = \Sigma_{p+a}(p) + \Sigma_{\mathrm{zm}}(p), \tag{22}$$

where $\Sigma_{p+a}(p)$ incorporates the contributions from the regions of integration over dx ($-\infty < x < \infty$), excluding the singular points $x = 0$ and $x = 1$, while the zero-mode part $\Sigma_{\mathrm{zm}}(p)$ involves the integrations in the ϵ-vicinities of these two points.

The calculation is carried out in Appendix B. After closing the integration contour by an arc of a circle (see Appendix B), the integral for $\Sigma_{p+a}(p)$ is represented as a sum of the pole and arc contributions and has the form

$$\Sigma_{p+a}(p) = -\frac{g^2}{16\pi^3}\int d^2k_\perp \int_\epsilon^{1-\epsilon} \frac{(\not p - \not k + m)dx}{\mathbf{k}_\perp^2 + m^2x - p^2x(1-x) + \mu^2(1-x)} + \frac{g^2 \not\omega}{32\pi^3(\omega\cdot p)}\int d^2k_\perp \int_{1+\epsilon}^{+\infty}\frac{dx}{x(1-x)}. \quad (23)$$

Comparing Eq. (23) with Eqs. (5), we see that

$$\Sigma_{p+a}(p) = \Sigma_{2b}(p) + \Sigma_{fc}(p), \quad (24)$$

where both terms on the right-hand side are regularized at $x = 0$ and $x = 1$. The pole plus arc contributions to Eq. (20) reproduce the result given by the sum of the two LFD diagrams shown in Fig. 1. Hence,

$$\Sigma_{p+a}(p) = g^2\left[\mathcal{A}(p^2) + \mathcal{B}(p^2)\frac{\not p}{m} + C_{p+a}\frac{m\not\omega}{\omega\cdot p}\right], \quad (25)$$

where $\mathcal{A}(p^2)$ and $\mathcal{B}(p^2)$ are defined by Eqs. (9a) and (9b), while C_{p+a} coincides with $\tilde{C}$, Eq. (10).

As mentioned above, the zero-mode contribution results from the divergence (at $L \to \infty$) of the integral over k_-, which occurs when $x = 0$, 1. This divergence is determined by the leading k_--term in the numerator of Eq. (20), that is by $\frac{1}{2}\gamma_+ k_-$. In explicitly covariant LFD, the matrix γ_+ turns into $\not\omega$. The zero-mode contribution is therefore

$$\Sigma_{\rm zm}(p) \equiv g^2 C_{\rm zm}\frac{m\not\omega}{\omega\cdot p}, \quad (26)$$

where $C_{\rm zm}$ is calculated in Appendix B and has the form

$$C_{\rm zm} = \frac{m^2-\mu^2}{16\pi^2 m}\log\frac{\Lambda_\perp}{m} + \frac{1}{32\pi^2 m}\left(m^2 - \mu^2 - 2\mu^2\log\frac{m}{\mu}\right). \quad (27)$$

We thus find

$$C_{p+a} + C_{\rm zm} = 0, \quad (28)$$

since $C_{p+a} = \tilde{C}$ is given by the right-hand side of Eq. (10). Substituting Eqs. (25) and (26) into Eq. (22), and taking into account Eq. (28), we finally get

$$\Sigma_F(p) = g^2\left[\mathcal{A}(p^2) + \mathcal{B}(p^2)\frac{\not p}{m}\right]. \quad (29)$$

We see that, after the incorporation of the pole, arc, and zero-mode contributions, the ω-dependent term in the self-energy disappears, even before the renormalization. Note that, although we used the same cutoffs, the formula (29) does not coincide with the expression (7) obtained by using the LFD graph technique rules, since the sum $\mathcal{C}(p^2) + C_{fc}$ is not zero [it is given by Eq. (10)]. One might think that the dependence of the self-energy (7) on ω is an artifact of the LFD rules, whereas the independence of the Feynman approach on ω is natural, since we started with the Feynman expression (19) which "knows nothing" about ω. It is not so, since the initially divergent integral for $\Sigma(p)$ acquires some sense only after regularization, and the latter has been done in terms of the cutoffs imposed on the LF variables. The independence of $\Sigma_F(p)$ on ω looks thereby as a coincidence. We shall see in Sec. III B that, in the EMV case, in contrast to the self-energy one, the LF cutoffs applied to the initial Feynman integral *do result in* some dependence of the EMV on the LF plane orientation.

After the renormalization, Eq. (29) reproduces the expression (16) obtained earlier for the self-energy found within LFD and regularized by the invariant PV method.

2. Invariant regularization

We briefly recall in this section familiar results known from the standard four-dimensional Feynman formalism which is completely independent from LFD. It may serve as an additional test of the results obtained above.

The fermion self-energy is given by Eq. (19). It is convenient to use the following decomposition:

$$\Sigma_F(p) = g^2\left[\mathcal{A}_F(p^2) + \mathcal{B}_F(p^2)\frac{\not p}{m}\right], \quad (30)$$

where $\mathcal{A}_F(p^2)$ and $\mathcal{B}_F(p^2)$ are scalar functions. Note that they do not coincide with $\mathcal{A}(p^2)$ and $\mathcal{B}(p^2)$ from Eq. (29), since we use here another regularization procedure. Applying the Feynman parametrization, we can rewrite Eq. (19) as

$$\Sigma_F(p) = \frac{ig^2}{16\pi^4}\int d^4k' \int_0^1 dx \frac{(1-x)\not p - \not k' + m}{[k'^2 - m^2x + p^2x(1-x) - \mu^2(1-x) + i0]^2}, \quad (31)$$

where we introduced $k' = k - xp$. Going over to Euclidean space by means of the Wick rotation $k'_0 = ik'_4$ with real k'_4 and regularizing the divergent integrals by an invariant cutoff $|k'^2| = \mathbf{k}'^2 + k_4'^2 < \Lambda^2$ (assuming that $\Lambda^2 \gg \{m^2, \mu^2, |p^2|\}$), we can perform the four-dimensional integration and get

$$\Sigma_F(p) = -\frac{g^2}{16\pi^2}\int_0^1 dx[(1-x)\not p + m]\left\{\log\left[\frac{\Lambda^2}{m^2x - p^2x(1-x) + \mu^2(1-x)}\right] - 1\right\}. \quad (32)$$

The terms of order $1/\Lambda^2$ and higher are omitted. Comparing the right-hand sides of Eqs. (30) and (32), we find

$$\mathcal{A}_F(p^2) = -\frac{m}{16\pi^2}\left(\log\frac{\Lambda^2}{m^2} - 1\right) + \frac{m}{16\pi^2}\int_0^1 dx \log\left[\frac{m^2x - p^2x(1-x) + \mu^2(1-x)}{m^2}\right], \tag{33a}$$

$$\mathcal{B}_F(p^2) = -\frac{m}{32\pi^2}\left(\log\frac{\Lambda^2}{m^2} - 1\right) + \frac{m}{16\pi^2}\int_0^1 dx(1-x) \log\left[\frac{m^2x - p^2x(1-x) + \mu^2(1-x)}{m^2}\right]. \tag{33b}$$

The renormalized self-energy $\Sigma_{F,\mathrm{ren}}(p)$ is found from Eq. (14), changing $\Sigma^{\mathrm{PV},b+f}(p)$ by $\Sigma_F(p)$. The corresponding renormalized functions $\mathcal{A}_{F,\mathrm{ren}}(p^2)$ and $\mathcal{B}_{F,\mathrm{ren}}(p^2)$ coincide with $\mathcal{A}_{\mathrm{ren}}(p^2)$ and $\mathcal{B}_{\mathrm{ren}}(p^2)$ given by Eqs. (18). We thus reproduce again Eq. (16) for $\Sigma_{F,\mathrm{ren}}(p)$.

It is easy to verify that using the PV subtraction for the boson propagator (instead of the cutoff Λ^2),

$$\Sigma_F^{\mathrm{PV},b}(p) = \Sigma_F(p, m, \mu) - \Sigma_F(p, m, \mu_1),$$

leads, in the limit $\mu_1 \to \infty$, to the same expression (16) for the renormalized self-energy. We have therefore

$$\Sigma_{F,\mathrm{ren}}(p) = \Sigma_{F,\mathrm{ren}}^{\mathrm{PV},b}(p) = \Sigma_{\mathrm{ren}}^{\mathrm{PV},b+f}(p). \tag{34}$$

To conclude, any of the considered ways of regularization (either with the noninvariant cutoffs $\Lambda_\perp$ and ϵ or with the single bosonic PV subtraction) can be used in order to get the correct expression for the renormalized self-energy in the Feynman approach, while the double (bosonic + fermionic) PV subtraction is required in the case of LFD.

III. FERMION ELECTROMAGNETIC VERTEX

We can now proceed to the calculation of the spin-1/2 fermion elastic EMV, Γ_ρ, which is connected with the matrix element of the electromagnetic current J_ρ by the relation

$$J_\rho = e\bar{u}(p')\Gamma_\rho u(p), \tag{35}$$

where e is the physical electromagnetic coupling constant, p and p' are the initial and final on-mass-shell fermion four-momenta ($p'^2 = p^2 = m^2$). Assuming P-, C-, and T-parity conservation, Γ_ρ is defined by two form factors depending on the momentum transfer squared $Q^2 = -(p'-p)^2$:

$$\bar{u}'\Gamma_\rho u = \bar{u}'\left[F_1(Q^2)\gamma_\rho + \frac{iF_2(Q^2)}{2m}\sigma_{\rho\nu}q_\nu\right]u. \tag{36}$$

We omit for simplicity the bispinor arguments and denoted $q = p' - p$, $\sigma_{\rho\nu} = i(\gamma_\rho\gamma_\nu - \gamma_\nu\gamma_\rho)/2$.

We consider here, as in Sec. II, the Yukawa model which takes into account interaction of fermions with scalar bosons, while the EMV "dressing" due to fermion-photon interactions is neglected. The fermion-boson interaction is treated perturbatively, up to terms of order g^2.

At that order, the EMV must be renormalized. The standard renormalization recipe consists in the subtraction $\Gamma_\rho^{\mathrm{ren}} = \Gamma_\rho - Z_1\gamma_\rho$ with the constant Z_1 found from the requirement $\bar{u}(p)\Gamma_\rho^{\mathrm{ren}}u(p) = \bar{u}(p)\gamma_\rho u(p)$. This leads to the following well-known expressions for the renormalized form factors:

$$F_1^{\mathrm{ren}}(Q^2) = 1 + F_1(Q^2) - F_1(0), \qquad F_2^{\mathrm{ren}}(Q^2) = F_2(Q^2). \tag{37}$$

We shall follow the same ideology that we exposed above for the self-energy: independent calculations of the EMV are performed, within covariant LFD and the Feynman approach, both for noninvariant and invariant regularization. However, in contrast to the self-energy case, the use of rotationally noninvariant cutoffs results in the appearance of new structures (and form factors) in the EMV, even if one starts from the standard four-dimensional Feynman expression. By this reason, the renormalization of the two physical form factors only, as prescribed by Eqs. (37), is not enough to get the full renormalized EMV.

A. Calculation in light-front dynamics

1. Light-front interaction Hamiltonian involving electromagnetic interaction

Before going over to the consideration of the EMV in covariant LFD, one should derive the interaction Hamiltonian which involves both fermion-boson and fermion-photon interactions. Although all the diagrams calculated below are generated by the graph technique rules formulated in Ref. [1], this is another way to explain their origin.

We will not give here a detailed derivation. The corresponding procedure is exposed in Ref. [7]. We derived there the LF Hamiltonian describing a system of interacting fermion and massless vector boson fields. This expression holds also for a fermion-photon system. When the photon field is taken in the Feynman gauge, the Hamiltonian in Schrödinger representation has the form

$$H^{\mathrm{int}}(x) = -e\bar{\psi}\not{A}\psi + e^2\bar{\psi}\not{A}\frac{\not{\omega}}{2i(\omega\cdot D_A)}\not{A}\psi, \tag{38}$$

where ψ and A are the free fermion and photon fields, respectively, and the operator $1/(i\omega\cdot D_A)$ in coordinate space acts on the coordinate along the four-vector ω (for convenience we denote it for a moment as x_-, since ω in standard LFD has only the minus-component):

$$\frac{1}{i\omega\cdot D_A}f(x_-) = \exp\left[-\frac{e}{i\omega\cdot\partial}\omega\cdot A\right]\frac{1}{i\omega\cdot\partial} \times\left\{\exp\left[\frac{e}{i\omega\cdot\partial}\omega\cdot A\right]f(x_-)\right\} \tag{39}$$

and $1/(i\omega\cdot\partial)$ is the free reversal derivative operator:

$$\frac{1}{i\omega\cdot\partial}f(x_-) = -\frac{i}{4}\int dy_- \epsilon(x_- - y_-) f(y_-), \qquad (40)$$

where $\epsilon(x)$ is the sign function. The operators $1/(i\omega\cdot\partial)$ inside the exponents act on the functions $\omega\cdot A$ only, while that standing between the exponents acts on all the functions to the right of it. In momentum representation, the action of the operator $1/(i\omega\cdot\partial)$ on a function $f(x)$ reduces to the multiplication of its Fourier transform $f(k)$ by the factor $1/(\omega\cdot k)$.

It is easy to modify the Hamiltonian (38) in order to incorporate interactions between fermions and scalar bosons. The equation of motion for the Heisenberg fermion field operator Ψ, in the absence of scalar bosons, looks like $(i\not\partial - m)\Psi = -e\not\mathcal{A}\Psi$, where $\mathcal{A}$ is the Heisenberg photon field operator. If we introduce a scalar boson field Φ, the equation of motion becomes $(i\not\partial - m)\Psi = (-e\not\mathcal{A} - g\Phi)\Psi$. Since the latter equation of motion is obtained from the previous one by the substitution $\not\mathcal{A} \to \not\mathcal{A} + (g/e)\Phi$, it is enough to make the same substitution in the Hamiltonian (38), everywhere except in the operator $1/(i\omega\cdot D_A)$ [7]. The Hamiltonian thus becomes

$$H^{\rm int}(x) = -\bar\psi[g\varphi + e\not A]\psi + \bar\psi[g\varphi + e\not A]\frac{\hat\omega}{2i\omega\cdot D_A} \times [g\varphi + e\not A]\psi. \qquad (41)$$

We see that the LFD interaction Hamiltonian (41) involves also, besides the usual term $-\bar\psi[g\varphi + e\not A]\psi$ describing ordinary fermion-boson and fermion-photon interactions, the so-called contact terms which are nonlinear in the coupling constants. Note that if we expand the Hamiltonian (41) in powers of e, this expansion contains an infinite number of terms. Such a peculiarity is connected with the photon spin and with the gauge we have chosen.

In this paper, we are not interested in studying electromagnetic effects, but focus on the interaction between fermions and scalar bosons. We therefore restrict the Hamiltonian to the first order in the electromagnetic coupling constant e, neglecting the terms of order e^2 and higher. The result is

$$H^{\rm int} = H_{fb1} + H_{fb2} + H_{\rm em1} + H_{\rm em2} + H_{\rm em3}, \qquad (42)$$

where

$$H_{fb1} = -g\bar\psi\psi\varphi, \qquad (43a)$$

$$H_{fb2} = g^2\bar\psi\varphi\frac{\not\omega}{2i\omega\cdot\partial}\varphi\psi, \qquad (43b)$$

$$H_{\rm em1} = -e\bar\psi\not A\psi, \qquad (43c)$$

$$H_{\rm em2} = eg\bar\psi\left(\varphi\frac{\not\omega}{2i\omega\cdot\partial}\not A + \not A\frac{\not\omega}{2i\omega\cdot\partial}\varphi\right)\psi, \qquad (43d)$$

$$H_{\rm em3} = \frac{1}{2}eg^2\bar\psi\varphi\left\{\frac{\not\omega}{i\omega\cdot\partial}\left[\frac{1}{i\omega\cdot\partial}\omega\cdot A\right] - \left[\frac{1}{i\omega\cdot\partial}\omega\cdot A\right]\frac{\not\omega}{i\omega\cdot\partial}\right\}\varphi\psi. \qquad (43e)$$

The contact terms are H_{fb2}, $H_{\rm em2}$, and $H_{\rm em3}$. The operators $1/(i\omega\cdot\partial)$ inside the squared brackets act on $\omega\cdot A$ only.

2. Light-front diagrams and their amplitudes

Since the amplitude of the process which we are interested in is proportional to eg^2, we should collect together the matrix elements from the Hamiltonian (42) in the first, second and third orders of perturbation theory. It can be written schematically as

$$\langle H_{fb1}^2 H_{\rm em1}\rangle + \langle H_{fb1}H_{\rm em2}\rangle + \langle H_{\rm em3}\rangle.$$

Note that although the matrix element of the second order of perturbation theory, $\langle H_{fb2}H_{\rm em1}\rangle$, is also of order eg^2, it does not result in irreducible diagrams. The Hamiltonian (42) produces therefore the five contributions to the EMV, shown in Figs. 2–5. The triangle and pair creation diagrams are generated by $\langle H_{fb1}^2 H_{\rm em1}\rangle$, the left and right contact terms come from $\langle H_{fb1}H_{\rm em2}\rangle$, while $\langle H_{\rm em3}\rangle$ is responsible for the double contact term. Applying the rules

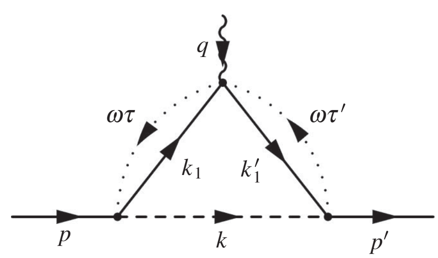

FIG. 2. Triangle LF diagram.

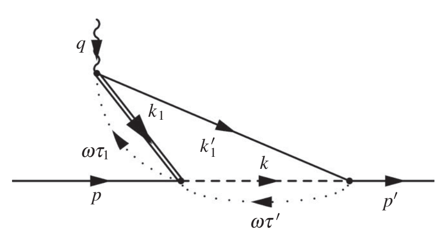

FIG. 3. Pair creation by a photon. The double solid line stands for an antifermion.

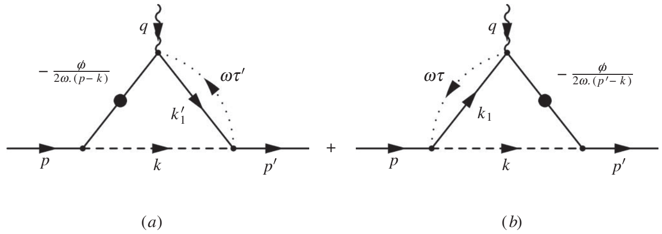

FIG. 4. Left (a) and right (b) contact terms.

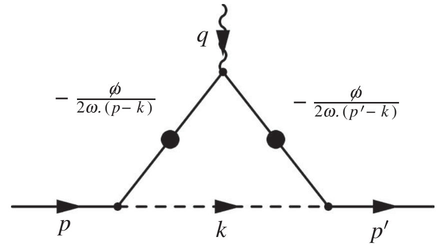

FIG. 5. Double contact term.

of the LFD graph technique [1] to these diagrams,[1] we can find analytical expressions for the corresponding amplitudes. However, before writing them down, one should note the following. When calculating the form factors in covariant LFD, the condition $\omega\cdot q = 0$ on the momentum transfer is usually imposed (equivalent to $q_+ = q_0 + q_z = 0$ in the noncovariant version of LFD). It comes from the analysis of the pure scalar "EMV" (i.e., when all the particles, including the photon, are spinless), where it forbids the pair creation diagram. Indeed, since the plus component of the pair momentum is always positive, the pair cannot be created by a virtual photon with $q_+ = 0$. As a result, when $q_+ \to 0$, the corresponding phase space volume tends to zero, and the amplitude of the pair creation diagram disappears. For systems involving fermions and/or vector photons, the amplitude of the pair creation diagram becomes indefinite if $\omega\cdot q$ exactly equals zero, since it is given by an integral with an infinitely large integrand and zero phase space volume. For this reason, one has to take $\omega\cdot q \neq 0$. We set $\omega\cdot q \equiv \alpha(\omega\cdot p)$, where α is a constant which we take positive, for definiteness. We will see below that, for the rotationally noninvariant cutoffs discussed in Sec. II, a nonzero contribution to the EMV from the pair creation diagram survives, and moreover, it tends to infinity when $\alpha \to 0$.

We can now proceed to the calculation of the LF diagram amplitudes. The contribution of the triangle diagram on Fig. 2 reads

$$\Gamma_\rho^{(\mathrm{tri})} = \frac{g^2}{(2\pi)^3}\int \theta(\omega\cdot k)\delta(k^2-\mu^2)d^4k(\not p' - \not k + \not\omega\tau' + m)\theta[\omega\cdot(p'-k)]\delta[(p'-k+\omega\tau')^2 - m^2]\frac{d\tau'}{\tau'}$$
$$\times \gamma_\rho(\not p - \not k + \not\omega\tau + m)\theta[\omega\cdot(p-k)]\delta[(p-k+\omega\tau)^2-m^2]\frac{d\tau}{\tau}$$
$$= \frac{g^2}{(2\pi)^3}\int d^2k_\perp\int_\epsilon^{1-\epsilon}\frac{dx}{2x}\frac{(\not p' - \not k + \not\omega\tau' + m)\gamma_\rho(\not p - \not k + \not\omega\tau + m)}{2\omega\cdot(p'-k)\tau' 2\omega\cdot(p-k)\tau}. \tag{44}$$

We have introduced here new integration LF variables $\mathbf{k}_\perp$ and x in a standard fashion (see Sec. II A 1). The singularities of the integrand at $x = 0$ and $x = 1$ are excluded by introducing an infinitesimal positive cutoff ϵ. The values of τ's are found from the conservation laws imposed by the delta functions. Namely,

$$2\omega\cdot(p-k)\tau = m^2 - (p-k)^2 = (1-x)\left(\frac{\mathbf{k}_\perp^2 + m^2}{1-x} + \frac{\mathbf{k}_\perp^2+\mu^2}{x} - m^2\right), \tag{45a}$$

$$2\omega\cdot(p'-k)\tau' = m^2 - (p'-k)^2 = (1-x')\left(\frac{\mathbf{k}_\perp'^2 + m^2}{1-x'} + \frac{\mathbf{k}_\perp'^2+\mu^2}{x'} - m^2\right), \tag{45b}$$

where $x' = \omega\cdot k/\omega\cdot p' = x/(1+\alpha)$, $\mathbf{k}'_\perp = \mathbf{k}_\perp - x'\mathbf{\Delta}$, and $\mathbf{\Delta}$ is the part of the three-vector $\mathbf{q}$, transversal to $\boldsymbol{\omega}$. Note that

$$\mathbf{\Delta}^2 = Q^2(1+\alpha) - \alpha^2 m^2. \tag{46}$$

The formulas (45) and (46) follow from the kinematical relations listed in Appendix A.

The contribution of the pair creation diagram, Fig. 3, is given by

[1]The rules incorrectly prescribe to use the theta function $\theta(\omega\cdot k)$ for the contact term. This theta function should be removed.

$$\Gamma_\rho^{(\mathrm{pair})} = \frac{g^2}{(2\pi)^3}\int \theta(\omega\cdot k)\delta(k^2-\mu^2)d^4k(\not p' - \not k + \not\omega\tau' + m)\theta[\omega\cdot(p'-k)]\delta[(p'-k+\omega\tau')^2-m^2]\frac{d\tau'}{\tau'}$$
$$\times \gamma_\rho(\not p - \not k + \not\omega\tau' - \not\omega\tau_1 + m)\theta[\omega\cdot(k-p)]\delta[(p-k+\omega\tau'-\omega\tau_1)^2-m^2]\frac{d\tau_1}{\tau_1}.$$

The line carrying the four-momentum k_1 corresponds to an antifermion and is described by the propagator $(m-\not k_1)\theta(\omega\cdot k_1)\delta(k_1^2-m^2)$. It is convenient to introduce a new variable $\tau = \tau' - \tau_1$, instead of τ_1:

$$\Gamma_\rho^{(\mathrm{pair})} = \frac{g^2}{(2\pi)^3}\int \frac{d^3k}{2\varepsilon_{\mathbf{k}}}(\not p' - \not k + \not\omega\tau' + m)\theta[\omega\cdot(p'-k)]\delta[(p'-k+\omega\tau')^2-m^2]\frac{d\tau'}{\tau'}\gamma_\rho(\not p - \not k + \not\omega\tau + m)$$
$$\times\theta[\omega\cdot(k-p)]\delta[(p-k+\omega\tau)^2-m^2]\frac{d\tau}{(\tau'-\tau)}$$
$$= -\frac{g^2}{(2\pi)^3}\int d^2k_\perp\int_{1+\epsilon}^{1+\alpha-\epsilon}\frac{dx}{2x}\frac{(\not p' - \not k + \not\omega\tau' + m)\gamma_\rho(\not p - \not k + \not\omega\tau + m)}{2\omega\cdot(p'-k)\tau' 2\omega\cdot(p-k)(\tau'-\tau)}. \tag{47}$$

The "shifted" τ enters the delta function and is determined by the same formula (45a) as τ in other Γ's. We can therefore use the same kinematics. The integration over $d\tau$ by means of the delta function $\delta[(p-k+\omega\tau)^2-m^2]$ brings the factor $|\omega\cdot(p-k)|$ in the denominator. We used that $|\omega\cdot(p-k)| = -\omega\cdot(p-k)$ inside the integration interval $1+\epsilon < x < 1+\alpha-\epsilon$.

The contribution of the left contact term to the EMV is shown in Fig. 4(a). The corresponding amplitude has the form

$$\Gamma_\rho^{(\mathrm{lct})} = \frac{g^2}{(2\pi)^3}\int \theta(\omega\cdot k)\delta(k^2-\mu^2)d^4k(\not p' - \not k + \not\omega\tau' + m)\theta[\omega\cdot(p'-k)]\delta[(p'-k+\omega\tau')^2-m^2]$$
$$\times\frac{d\tau'}{\tau'}\gamma_\rho\left[-\frac{\not\omega}{2\omega\cdot(p-k)}\right]$$
$$= -\frac{g^2}{(2\pi)^3}\int d^2k_\perp\int_\epsilon^{1+\alpha-\epsilon}\frac{dx}{2x}\frac{(\not p' - \not k + \not\omega\tau' + m)\gamma_\rho\not\omega}{2\omega\cdot(p'-k)\tau' 2\omega\cdot(p-k)}. \tag{48}$$

For the right contact term, Fig. 4(b), we get

$$\Gamma_\rho^{(\mathrm{rct})} = \frac{g^2}{(2\pi)^3}\int \theta(\omega\cdot k)\delta(k^2-\mu^2)d^4k\left[-\frac{\not\omega}{2\omega\cdot(p'-k)}\right]\gamma_\rho(\not p - \not k + \not\omega\tau + m)\theta[\omega\cdot(p-k)]\delta[(p-k+\omega\tau)^2-m^2]\frac{d\tau}{\tau}$$
$$= -\frac{g^2}{(2\pi)^3}\int d^2k_\perp\int_\epsilon^{1-\epsilon}\frac{dx}{2x}\frac{\not\omega\gamma_\rho(\not p - \not k + \not\omega\tau + m)}{2\omega\cdot(p'-k)2\omega\cdot(p-k)\tau}. \tag{49}$$

Finally, the double contact term, Fig. 5, yields

$$\Gamma_\rho^{(2\mathrm{ct})} = \frac{g^2}{(2\pi)^3}\int d^2k_\perp\int_\epsilon^{+\infty}\frac{dx}{2x}$$
$$\times\frac{\not\omega}{2\omega\cdot(p'-k)}\gamma_\rho\frac{\not\omega}{2\omega\cdot(p-k)}. \tag{50}$$

The full EMV is the sum of all the five contributions (44) and (47)–(50). Note that the limits of integrations over dx are different in these contributions. In order to make the calculations easier, we split the whole region of possible values of x into the three subregions: (i) $\epsilon < x < 1-\epsilon$; (ii) $1+\epsilon < x < 1+\alpha-\epsilon$; (iii) $1+\alpha+\epsilon < x < +\infty$. We then represent each of the vertices $\Gamma_\rho^{(\mathrm{lct})}$ and $\Gamma_\rho^{(2\mathrm{ct})}$ as a sum of integrals over these integration subregions, removing the singularities by means of the same cutoff ϵ:

$$\Gamma_\rho^{(\mathrm{lct})} = \Gamma_\rho^{(1,\mathrm{lct})} + \Gamma_\rho^{(2,\mathrm{lct})},$$

where

$$\Gamma_\rho^{(1,\mathrm{lct})} = -\frac{g^2}{64\pi^3}\frac{1}{(\omega\cdot p)^2}\int d^2k_\perp\int_\epsilon^{1-\epsilon}\frac{dx}{x}$$
$$\times\frac{(\not p' - \not k + \not\omega\tau' + m)\gamma_\rho\not\omega}{(1+\alpha-x)(1-x)\tau'},$$
$$\Gamma_\rho^{(2,\mathrm{lct})} = -\frac{g^2}{64\pi^3}\frac{1}{(\omega\cdot p)^2}\int d^2k_\perp\int_{1+\epsilon}^{1+\alpha-\epsilon}\frac{dx}{x}$$
$$\times\frac{(\not p' - \not k + \not\omega\tau' + m)\gamma_\rho\not\omega}{(1+\alpha-x)(1-x)\tau'},$$

and, analogously,

$$\Gamma_\rho^{(2\mathrm{ct})} = \Gamma_\rho^{(1,2\mathrm{ct})} + \Gamma_\rho^{(2,2\mathrm{ct})},$$

where

$$\Gamma_\rho^{(1,2ct)} = \frac{g^2}{64\pi^3}\frac{\not\omega\gamma_\rho\not\omega}{(\omega\cdot p)^2} \times \int d^2k_\perp \int_\epsilon^{1-\epsilon}\frac{dx}{x(1+\alpha-x)(1-x)},$$

$$\Gamma_\rho^{(2,2ct)} = \frac{g^2}{64\pi^3}\frac{\not\omega\gamma_\rho\not\omega}{(\omega\cdot p)^2} \times \int d^2k_\perp \int_{1+\epsilon}^{1+\alpha-\epsilon}\frac{dx}{x(1+\alpha-x)(1-x)} + \frac{g^2}{64\pi^3}\frac{\not\omega\gamma_\rho\not\omega}{(\omega\cdot p)^2} \times \int d^2k_\perp \int_{1+\alpha+\epsilon}^{\infty}\frac{dx}{x(1+\alpha-x)(1-x)}.$$

After some rearrangement of the contributions, we can represent the full EMV as

$$\Gamma_\rho \equiv \Gamma_\rho^{(A)} + \Gamma_\rho^{(B)} + \Gamma_\rho^{(C)} \tag{51}$$

with

$$\Gamma_\rho^{(A)} = \Gamma_\rho^{(tri)} + \Gamma_\rho^{(1,lct)} + \Gamma_\rho^{(rct)} + \Gamma_\rho^{(1,2ct)} - \Gamma_\rho^{(0)}, \tag{52a}$$

$$\Gamma_\rho^{(B)} = \Gamma_\rho^{(pair)} + \Gamma_\rho^{(2,lct)} - \Gamma_\rho^{(1)}, \tag{52b}$$

$$\Gamma_\rho^{(C)} = \Gamma_\rho^{(2,2ct)} + \Gamma_\rho^{(0)} + \Gamma_\rho^{(1)}. \tag{52c}$$

The two new integrals,

$$\Gamma_\rho^{(0)} = \frac{g^2}{64\pi^3(1+\alpha)}\frac{\not\omega\gamma_\rho\not\omega}{(\omega\cdot p)^2}\int d^2k_\perp\int_\epsilon^{1-\epsilon}\frac{dx}{x}, \tag{53a}$$

$$\Gamma_\rho^{(1)} = \frac{g^2}{64\pi^3\alpha}\frac{\not\omega\gamma_\rho\not\omega}{(\omega\cdot p)^2}\int d^2k_\perp\int_{1+\epsilon}^{1+\alpha-\epsilon}\frac{dx}{x(1+\alpha-x)} \tag{53b}$$

have been introduced in order to make the integrands of $\Gamma_\rho^{(A)}$ and $\Gamma_\rho^{(B)}$ nonsingular in x, although each term on the right-hand sides of Eqs. (52a) and (52b) contains logarithmic divergencies either at $x=0$ or at $x=1$, or at $x=1+\alpha$.

Taking the sums (52a) and (52b), we easily find

$$\Gamma_\rho^{(A)} = \frac{g^2}{16\pi^3}\int d^2k_\perp\int_0^1\frac{dx}{x}\left[\frac{(\not p'-\not k+m)\gamma_\rho(\not p-\not k+m)}{(\mu^2-2p'\cdot k)(\mu^2-2p\cdot k)} - \frac{\not\omega\gamma_\rho\not\omega}{4(1+\alpha)(\omega\cdot p)^2}\right], \tag{54a}$$

$$\Gamma_\rho^{(B)} = \frac{g^2}{64\pi^3(\omega\cdot p)^2}\int d^2k_\perp\int_1^{1+\alpha}\frac{dx}{x(1+\alpha-x)}\left[\frac{(\not p'-\not k+\not\omega\tau'+m)\gamma_\rho(\not p-\not k+\not\omega\tau'+m)}{(x-1)\tau'(\tau'-\tau)} - \frac{\not\omega\gamma_\rho\not\omega}{\alpha}\right]. \tag{54b}$$

Since the regularization in x is no more required, we set $\epsilon = 0$.

The remaining part of the EMV, $\Gamma_\rho^{(C)}$, is given by a sum of regularized integrals:

$$\Gamma_\rho^{(C)} = \frac{g^2}{64\pi^3}\frac{\not\omega\gamma_\rho\not\omega}{(\omega\cdot p)^2}\int d^2k_\perp\left[\frac{1}{1+\alpha}\int_\epsilon^{1-\epsilon}\frac{dx}{x} + \frac{1}{\alpha}\int_{1+\epsilon}^{1+\alpha-\epsilon}\frac{dx}{x(1-x)} + \int_{1+\alpha+\epsilon}^{+\infty}\frac{dx}{x(1+\alpha-x)(1-x)}\right]. \tag{55}$$

3. *Electromagnetic form factors*

We represent the EMV via the following decomposition:

$$\bar u'\Gamma_\rho u = \bar u'\left\{F_1\gamma_\rho + \frac{iF_2}{2m}\sigma_{\rho\nu}q_\nu + B_1\left[\frac{\not\omega}{\omega\cdot p}(p+p')_\rho - 2\gamma_\rho\right] + B_2\frac{m\omega_\rho}{\omega\cdot p} + B_3\frac{m^2\not\omega\omega_\rho}{(\omega\cdot p)^2}\right\}u, \tag{56}$$

which is similar, although not identical, to the one used in Ref. [20]. We shall come back to this difference in Sec. IV. The decomposition is determined by the five[2] form factors $F_{1,2}$, B_{1-3}. We shall call $F_{1,2}$ the physical form factors, in contrast to the nonphysical ones, B_{1-3}, which must be absent in the physically observed EMV. The appearance of the three extra form factors is a property of LFD. Note that they appear in standard noncovariant LFD as well, but in this approach they cannot be separated out from the physical form factors, and an illusion may occur that the EMV structure is determined, according to Eq. (36), by the two form factors, as in the Feynman case. This is however not so, because the electromagnetic current operator in LFD has *five* independent matrix elements, not two. One may argue that, even if each particular LF diagram produces a contribution of the form (56) to the EMV, the extra three structures disappear (i.e., one has $B_{1-3}=0$) after summing up all the contributions, at least in a given order of perturbation theory. It would be so if the amplitudes of the LF diagrams were given by convergent integrals, which happens for the pure scalar case (scalar bosons plus scalar "photon" and no fermions). For systems involving fermions, however, the amplitudes strongly diverge. Their regularization, as will be shown below, may give rise to the appearance of extra (ω-dependent) spin structures in the perturbative and nonperturbative regularized EMV's. In

[2] The coincidence of the number of form factors with the number of LF diagrams is, of course, by chance.

this sense the situation is analogous to the case of the fermion self-energy discussed in the previous section.

The procedure to calculate the form factors is quite similar to that exposed in Ref. [20]. We define the matrix

$$O_\rho = \frac{(\not p' + m)\Gamma_\rho(\not p + m)}{4m^2} \tag{57}$$

and the following contractions:

$$c_1 = \mathrm{Tr}\{O_\rho \gamma^\rho\}, \qquad c_2 = \frac{iq_\nu}{2m}\mathrm{Tr}\{O_\rho \sigma^{\rho\nu}\},$$
$$c_3 = \frac{(p+p')^\rho}{\omega\cdot p}\mathrm{Tr}\{O_\rho \not\omega\}, \qquad c_4 = \frac{m\omega^\rho}{\omega\cdot p}\mathrm{Tr}\{O_\rho\}, \tag{58}$$
$$c_5 = \frac{m^2\omega^\rho}{(\omega\cdot p)^2}\mathrm{Tr}\{O_\rho \not\omega\}.$$

Now, using Eq. (56), we can get the following relations between the form factors and the quantities c_{1-5}:

$$\begin{aligned}
c_1 &= (2-4\eta)F_1 - 6\eta F_2 + 2(4\eta+\alpha)B_1 + (2+\alpha)B_2 \\
&\quad + 2(1+\alpha)B_3, \\
c_2 &= 6\eta F_1 + 2\eta(2-\eta)F_2 - 2\eta(4-\alpha)B_1 \\
&\quad + \eta(2+\alpha)B_2 + \frac{\alpha^2}{2}B_3, \\
c_3 &= 2(2+\alpha)F_1 - 2\eta(2+\alpha)F_2 + 4[2\eta(1+\alpha)+\alpha]B_1 \\
&\quad + (2+\alpha)^2 B_2 + 2(2+\alpha)(1+\alpha)B_3, \\
c_4 &= (2+\alpha)[F_1 - \eta F_2 + \alpha B_1], \\
c_5 &= 2(1+\alpha)F_1 - \frac{\alpha^2}{2}F_2 + 2\alpha(1+\alpha)B_1,
\end{aligned} \tag{59}$$

where $\eta = Q^2/(4m^2)$. Solving the system of linear equations (59) with respect to $F_{1,2}$ and B_{1-3}, we express them through c_{1-5}. These expressions are lengthy and we do not give them here. Then, substituting formulas (54) and (55) for $\Gamma_\rho^{(A)}$, $\Gamma_\rho^{(B)}$, and $\Gamma_\rho^{(C)}$ into Eq. (57), calculating the traces (58), and expressing the scalar products of the four-vectors p, p', k, and ω through the two-dimensional vectors $\mathbf{k}_\perp$, $\mathbf{\Delta}$, and the scalars x, α, we cast each form factor in the form of a three-dimensional integral over $d^2k_\perp dx$. The expressions for the scalar products through the integration variables and the momentum transfer are given in Appendix A.

4. Regularization with rotationally noninvariant cutoffs

We give here the final expressions for the form factors found by using the rotationally noninvariant cutoffs $\Lambda_\perp$ and ϵ imposed on the variables $|\mathbf{k}_\perp|$ and x. As we said above, the vertex functions $\Gamma_\rho^{(A)}$ and $\Gamma_\rho^{(B)}$ do not require to introduce a cutoff in x. As far as $\Gamma_\rho^{(C)}$ is concerned, it is represented by a sum of integrals, each requiring regularization and thus depending on ϵ. However, as can be established by direct integration in Eq. (55), the sum itself has a finite limit when $\epsilon \to 0$:

$$\Gamma_\rho^{(C)} = \frac{g^2\Lambda_\perp^2}{32\pi^2}\frac{\log(1+\alpha)}{\alpha(1+\alpha)}\frac{\not\omega\omega_\rho}{(\omega\cdot p)^2}. \tag{60}$$

We therefore remain with the cutoff $\Lambda_\perp$ only. Note that the mutual cancellation of the terms singular in x, which happens for the full EMV, is connected with rather weak (logarithmic) divergence of the corresponding integrals, so that the cutoff $\Lambda_\perp$ is enough to make them finite. The same took place in the fermion self-energy case (see Sec. II A 2). As we shall see below [Eq. (C11) in Appendix C], the quadratically divergent term $\sim\not\omega\omega_\rho\Lambda_\perp^2$ results also from $\Gamma_\rho^{(B)}$ (but not from $\Gamma_\rho^{(A)}$) and cancels in the sum with $\Gamma_\rho^{(C)}$.

The details of calculations of all the contributions (A, B, C) are given in Appendix C. Adding all of them together, we arrive at the following final result for the form factors:

$$F_1 = \frac{g^2}{16\pi^2}\log\frac{\Lambda_\perp}{m} + \frac{g^2}{4\pi^2}\left(\log\frac{m}{\mu} - \frac{7}{8}\right) - \frac{g^2Q^2}{24\pi^2m^2}\left(\log\frac{m}{\mu} - \frac{9}{8}\right) + O(Q^4), \tag{61a}$$

$$F_2 = \frac{3g^2}{16\pi^2} - \frac{g^2Q^2}{32\pi^2m^2} + O(Q^4), \tag{61b}$$

$$B_1 = -\frac{g^2}{64\pi^2}, \tag{61c}$$

$$B_2 = -\frac{g^2}{32\pi^2}, \tag{61d}$$

$$B_3 = -\frac{g^2(m^2-\mu^2)}{16\pi^2m^2}\log\frac{\Lambda_\perp}{m} + \frac{g^2}{32\pi^2m^2}\left[\frac{Q^2}{\alpha} + \mu^2\left(2\log\frac{m}{\mu} + 1\right)\right]. \tag{61e}$$

Note that the terms $\sim\log\frac{\Lambda_\perp}{m}$ cancel in the form factors B_1 and B_2. These form factors are finite and do not depend on any cutoff, in contrast to B_3 which does not have a finite limit when $\Lambda_\perp \to \infty$. As we have already mentioned, neither of the form factors depend on the cutoff ϵ. At the same time, the amplitude of each of the LF diagrams shown in Figs. 2–5, diverges like $\Lambda_\perp^2\log\epsilon$. It means that the senior divergent terms $\sim\Lambda_\perp^2\log\epsilon$ and $\sim\Lambda_\perp^2$ cancel after the incorporation of all the LF diagrams. However, the form factors B_{1-3} which must be absent in the physical EMV remain nonzero values. The same happened for the $\sim\not\omega$ term in the full self-energy, Eq. (7).

We also see that B_3 has a pole at $\alpha = 0$. One cannot set here $Q^2 = 0$, since it is impossible to keep fixed $\alpha = (\omega\cdot q)/(\omega\cdot p)$ when $q \to 0$. More precisely, since $\mathbf{\Delta}^2 \geq 0$, from Eq. (46) we have $Q^2 \geq \frac{\alpha^2m^2}{1+\alpha}$. However, nothing prevents us to take $\alpha \to 0$ at fixed Q^2. As the inspection shows, the singular term $\sim 1/\alpha$ in B_3 results from $\Gamma_\rho^{(\mathrm{pair})}$, Eq. (47).

The standard renormalization procedure (37) affects the form factor F_1 only, so that

$$F_1^{\rm ren} = 1 - \frac{g^2 Q^2}{24\pi^2 m^2}\left(\log\frac{m}{\mu} - \frac{9}{8}\right) + O(Q^4). \tag{62}$$

The cutoff-dependent term $\sim \log(\Lambda_\perp/m)$ cancels, as it should. The renormalized form factor $F_2^{\rm ren}$ coincides with F_2, Eq. (61b). It is important to note that, in order to eliminate the three extra form factors B_{1-3}, one should introduce new ω-dependent counterterms into the interaction Hamiltonian. Since B_3 nontrivially depends on q through $Q^2 = -q^2$ and $\alpha = \omega\cdot q/\omega\cdot p$, its decomposition in powers of q contains an infinite number of terms. Therefore, to eliminate B_3 we need an infinite number of local counterterms, for this particular type of regularization.

5. Invariant Pauli-Villars regularization

We can now calculate the form factors within LFD, but using the invariant PV regularization instead of the LF cutoffs $\Lambda_\perp$ and ϵ.

Regularization by a PV boson.—We start with the regularization by one PV boson only. Since each of the LF diagrams contains one bosonic propagator, this regularization reduces to a simple subtraction

$$\mathcal{F}^{\rm PV,b} = \mathcal{F}(Q^2, m, \mu) - \mathcal{F}(Q^2, m, \mu_1).$$

As before, $\mathcal{F}$ denotes any of the form factors F_i or B_i. In the limit of large μ_1 we have

$$F_1(Q^2, m, \mu_1) = \frac{g^2}{16\pi^2}\log\frac{\Lambda_\perp}{m} - \frac{g^2}{16\pi^2}\left(\log\frac{\mu_1}{m} - \frac{1}{4}\right),$$
$$F_2(Q^2, m, \mu_1) = 0,$$

for arbitrary finite Q^2. Subtracting these expressions from those given by Eqs. (61a) and (61b), respectively, we get

$$F_1^{\rm PV,b} = \frac{g^2}{16\pi^2}\log\frac{\mu_1}{m} + \frac{g^2}{4\pi^2}\left(\log\frac{m}{\mu} - \frac{15}{16}\right) - \frac{g^2 Q^2}{24\pi^2 m^2}\left(\log\frac{m}{\mu} - \frac{9}{8}\right) + O(Q^4), \tag{63a}$$

$$F_2^{\rm PV,b} = \frac{3g^2}{16\pi^2} - \frac{g^2 Q^2}{32\pi^2 m^2} + O(Q^4). \tag{63b}$$

In spite of the fact that Eq. (63a) differs from Eq. (61a), both equations lead to the same renormalized form factor $F_1^{\rm ren}$, Eq. (62). The renormalized physical form factors obtained for the invariant and noninvariant types of regularization do therefore coincide.

Concerning the nonphysical form factors, the situation is quite different. Since B_{1-3} were calculated for arbitrary μ, we find from Eqs. (61c)–(61e)

$$B_1^{\rm PV,b} = B_2^{\rm PV,b} = 0, \tag{64a}$$

$$B_3^{\rm PV,b} = -\frac{g^2(\mu_1^2 - \mu^2)}{16\pi^2 m^2(1+\alpha)}\log\frac{\Lambda_\perp}{m} - \frac{g^2}{32\pi^2 m^2}\left(\mu_1^2 - \mu^2 - 2\mu^2\log\frac{m}{\mu} - 2\mu_1^2\log\frac{\mu_1}{m}\right). \tag{64b}$$

The formulas (63) are valid for $\mu \to 0$ and $\mu_1 \to \infty$, while Eqs. (64) hold for arbitrary μ and μ_1. The nonphysical form factors $B_{1,2}$ turned into zero, while $B_3^{\rm PV,b} \neq 0$ and still diverges logarithmically.

Regularization by one PV boson plus one PV fermion.—Since the PV regularization by one boson only does not cancel the form factor B_3, we have to introduce in addition a PV fermion. In that case, no contact terms appear at all, and the only diagrams which contribute to the EMV are the triangle (Fig. 2) and pair creation (Fig. 3) diagrams. Each of them contains two fermion propagators, both being subject to the PV regularization. For this reason we need to know the vertex with different internal fermions. We denote the masses of these fermions by m_i and $m_{i'}$, with the indices i and i' being either 0 or 1. Let $m_0 \equiv m$ and m_1 be the physical and PV fermion masses, respectively. Analogously, we denote the physical and PV boson masses by $\mu_0 \equiv \mu$ and μ_1.

The PV-regularized EMV is defined by

$$\Gamma_\rho^{\rm PV,b+f} = \sum_{i,i',j=0}^{1}(-1)^{i+i'+j}\Gamma_\rho(m_i, m_{i'}, \mu_j),$$

where the notation $\Gamma_\rho(m_i, m_{i'}, \mu_j)$ stands for the corresponding initial EMV calculated for the internal particles with the masses m_i, $m_{i'}$, and μ_j. The quantity $\Gamma_\rho(m_i, m_{i'}, \mu_j)$ itself is given by a sum of Eqs. (54), changing everywhere

$$\not p - \not k + m \to \not p - \not k + m_i,$$
$$\not p' - \not k + m \to \not p' - \not k + m_{i'},$$
$$\tau \to \frac{m_i^2 - (p-k)^2}{2\omega\cdot(p-k)},$$
$$\tau' \to \frac{m_{i'}^2 - (p'-k)^2}{2\omega\cdot(p'-k)},$$

and $\mu \to \mu_j$. The vertex $\Gamma_\rho^{(C)}$, Eq. (55), turns into zero already by the boson PV regularization and does not contribute to the PV-regularized form factors.

It can be shown that we do not need to introduce the PV fermion to regularize the form factors $F_{1,2}$ and $B_{1,2}$. In other words, in the limit $m_1 \to \infty$ we would obtain the same formulas (63) and (64a) as without the PV fermion at all. So, the only thing to do is to calculate $B_3^{\rm PV,b+f}$. This calculation is in principle quite similar to that performed above, but the algebra is more lengthy. We represent $B_3^{\mathrm{PV},b+f}$ as follows:

$$B_3^{\mathrm{PV},b+f} = \sum_{i,i'=0}^{1} (-1)^{i+i'} \sum_{N=A,B} B_3^{(N)\mathrm{PV},b}(m_i, m_{i'}), \tag{65}$$

where

$$B_3^{(N)\mathrm{PV},b}(m_i, m_{i'}) = \sum_{j=0}^{1} (-1)^j B_3^{(N)}(m_i, m_{i'}, \mu_j) \tag{66}$$

and $B_3^{(N)}(m_i, m_{i'}, \mu_j)$ is found through the vertex $\Gamma_\rho^{(N)}(m_i, m_{i'}, \mu_j)$. Though the order of summations in Eqs. (65) and (66) does not matter, it is convenient to calculate first $B_3^{(N)\mathrm{PV},b}(m_i, m_{i'})$, separately for the two vertices, then add the results, and finally sum over the PV fermion indices. Omitting rather tiresome manipulations, we give here the expressions for the functions $B_3^{(N)\mathrm{PV},b}(m_i, m_{i'})$, in order to see the details of the cancellations:

$$B_3^{(A)\mathrm{PV},b}(m_i, m_{i'}) = -\frac{g^2(\mu_1^2 - \mu^2)(2+\alpha)}{16\pi^2 m^2 (1+\alpha)^2} \log\frac{\Lambda_\perp}{m} + \frac{g^2}{32\pi^2 m^2}\left[2\mu_1^2 \log\frac{\mu_1}{m} + 2\mu^2 \log\frac{m}{\mu} - 3(\mu_1^2 - \mu^2)\right] + R(m_i, m_{i'}), \tag{67a}$$

$$B_3^{(B)\mathrm{PV},b}(m_i, m_{i'}) = \frac{g^2(\mu_1^2 - \mu^2)}{16\pi^2 m^2 (1+\alpha)^2} \log\frac{\Lambda_\perp}{m} + \frac{g^2(\mu_1^2 - \mu^2)}{16\pi^2 m^2} - R(m_i, m_{i'}), \tag{67b}$$

where

$$R(m_i, m_{i'}) = -\frac{g^2(\mu_1^2 - \mu^2)}{64\pi^2 m^2 Q^2}\left\{(m_i^2 - m_{i'}^2)\log\frac{m_i^2}{m_{i'}^2} - 2Q^2 \log\frac{m_i m_{i'}}{m^2} + s_Q \log\left[\frac{(m_i^2 - m_{i'}^2)^2 - (Q^2 - s_Q)^2}{(m_i^2 - m_{i'}^2)^2 - (Q^2 + s_Q)^2}\right]\right\}$$

and $s_Q = \sqrt{m_i^4 - 2m_i^2(m_{i'}^2 - Q^2) + (m_{i'}^2 + Q^2)^2}$. Both contributions (67) are rather complicated functions depending on the physical and PV masses, as well as on Q^2. In their sum, however, the dependence on the fermion mass m_1 and on Q^2 drops out completely, and for $\sum_{N=A,B} B_3^{(N)\mathrm{PV},b}(m_i, m_{i'})$ we arrive at the same expression (64b) found previously without any fermion PV regularization. The final summation over the fermion PV indices, as prescribed by Eq. (65), turns B_3 into zero:

$$B_3^{\mathrm{PV},b+f} = 0. \tag{68}$$

We can thus formulate the main results of this section: the full cancellation of the three nonphysical form factors is achieved by the double (i.e., bosonic + fermionic) PV regularization, whereas the single boson PV regularization cancels only two of the three nonphysical form factors. The renormalized physical form factors obtained by using the PV regularization (both single and double) coincide with those calculated through the rotationally noninvariant cutoffs.

B. Calculation in the four-dimensional Feynman approach

The amplitude of the Feynman triangle diagram which determines the EMV in the given order of perturbation theory is

$$\Gamma_\rho = \frac{ig^2}{(2\pi)^4}\int d^4k \frac{1}{[k^2 - \mu^2 + i0]} \times \frac{(\not p' - \not k + m)\gamma_\rho(\not p - \not k + m)}{[(p-k)^2 - m^2 + i0][p'-k)^2 - m^2 + i0]}, \tag{69}$$

where $p^2 = p'^2 = m^2$. As we shall see, the spin structure of the Feynman EMV depends on how it is regularized, in contrast to the self-energy, Eq. (19). In order to avoid overloading the formulas by additional indices indicating the type of the cutoffs, we use in this section the same notations for the Feynman EMV and the form factors as for the LFD ones.

1. Regularization with rotationally noninvariant cutoffs

As we did for the self-energy, Sec. II B 1, we first find the form factors by integrating the Feynman amplitude (69) in terms of the LF variables restricted by the transverse and longitudinal cutoffs. We shall see that such a procedure generates extra (nonphysical) form factors B_{1-3} [see Eq. (56)], in a very similar way as the use of the LFD rules.

Rewriting the integrand in Eq. (69) through the plus, minus, and transverse components of the four-vector k, we get

$$\Gamma_\rho = \frac{ig^2}{32\pi^4}\int d^2k_\perp dk_+ dk_- \frac{(\not p' - \not k + m)\gamma_\rho}{[(p'_+ - k_+)(p'_- - k_-) - (\mathbf{p}'_\perp - \mathbf{k}_\perp)^2 - m^2 + i0]} \times \frac{(\not p - \not k + m)}{[(p_+ - k_+)(p_- - k_-) - (\mathbf{p}_\perp - \mathbf{k}_\perp)^2 - m^2 + i0]}\frac{1}{[k_+k_- - \mathbf{k}_\perp^2 - \mu^2 + i0]}. \tag{70}$$

We take the reference frame where $\mathbf{p} = 0$. We then choose $p_+ = p'_+$. The latter condition is equivalent, in the language of covariant LFD, to $\alpha = (\omega\cdot q)/(\omega\cdot p) = 0$. In our LFD calculation of the form factors in Sec. III A, we initially kept α to be nonzero and went over to the limit $\alpha \to 0$ after summing up all the LF contributions. A smooth limit $\alpha \to 0$ was important in the LFD framework, since the amplitudes of different diagrams shown in Figs. 2–5 depend on α. The Feynman amplitude (69) is well defined for any values of its arguments p and p', in particular, for $p_+ = p'_+$. We can therefore safely set $p_+ - p'_+ = 0$ from the very beginning.

Similarly to Eq. (22) for the self-energy, we represent the full EMV as a sum of the two terms:

$$\Gamma_\rho \equiv \Gamma_\rho^{(p+a)} + \Gamma_\rho^{(zm)}, \tag{71}$$

corresponding to the "normal" contribution and the zero modes, respectively.

Like the self-energy case, the normal part $\Gamma_\rho^{(p+a)}$ is determined by the sum of the pole and arc contributions. It is calculated in Appendix D, Sec. D 2. The result reads

$$\Gamma_\rho^{(p+a)} = \frac{g^2}{16\pi^3}\int d^2k_\perp \int_0^1 \frac{dx}{x}\left[\frac{(\not p' - \not k + m)\gamma_\rho(\not p - \not k + m)}{(\mu^2 - 2p'\cdot k)(\mu^2 - 2p\cdot k)} - \frac{\not\omega\gamma_\rho\not\omega}{4(\omega\cdot p)^2}\right]. \tag{72}$$

Comparing the right-hand sides of Eq. (72) for $\Gamma_\rho^{(p+a)}$ and Eq. (54a) for the part $\Gamma_\rho^{(A)}$ of the EMV calculated within LFD, we see that they exactly coincide with each other at $\alpha = 0$:

$$\Gamma_\rho^{(p+a)} = \Gamma_\rho^{(A)}|_{\alpha=0}. \tag{73}$$

We have already encountered a similar situation above, in Sec. II B 1, where it was shown that the pole plus arc contribution to the Feynman expression for the self-energy exactly coincided with the full LFD self-energy [see Eq. (24)]. Evidently, the vertex $\Gamma_\rho^{(p+a)}$ can be also represented via form factors, in the form of the decomposition (56), but with its "own" form factors $F_{1,2}^{(p+a)}$, $B_{1-3}^{(p+a)}$. Form factors for $\Gamma_\rho^{(A)}$ were found in Appendix C. Because of the identity (73), in order to derive the form factors $F_{1,2}^{(p+a)}$ and $B_{1-3}^{(p+a)}$, we can make use of Eq. (C2) with the coefficients from Eqs. (C7)–(C9), taken at $\alpha = 0$. We thus find

$$F_1^{(p+a)} = \frac{g^2}{16\pi^2}\log\frac{\Lambda_\perp}{m} + \frac{g^2}{4\pi^2}\left(\log\frac{m}{\mu} - \frac{7}{8}\right) + \frac{g^2Q^2}{24\pi^2m^2}\left(\log\frac{m}{\mu} - \frac{9}{8}\right) + O(Q^4), \tag{74a}$$

$$F_2^{(p+a)} = \frac{3g^2}{16\pi^2} - \frac{g^2Q^2}{32\pi^2m^2} + O(Q^4), \tag{74b}$$

$$B_1^{(p+a)} = \frac{g^2}{16\pi^2}\log\frac{\Lambda_\perp}{m} - \frac{g^2}{64\pi^2} + \frac{g^2}{16\pi^2}\varphi(Q^2), \tag{74c}$$

$$B_2^{(p+a)} = -\frac{g^2}{8\pi^2}\log\frac{\Lambda_\perp}{m} - \frac{g^2}{32\pi^2} - \frac{g^2}{8\pi^2}\varphi(Q^2), \tag{74d}$$

$$B_3^{(p+a)} = -\frac{g^2}{32\pi^2m^2}(6m^2 - 4\mu^2 + Q^2)\log\frac{\Lambda_\perp}{m} + \frac{g^2}{32\pi^2m^2}\left[\mu^2\left(2\log\frac{m}{\mu} + 1\right) - (4m^2 - 2\mu^2 + Q^2)\varphi(Q^2)\right], \tag{74e}$$

where the function $\varphi(Q^2)$ is given by Eq. (C10). Note that $\varphi(0) = 0$. As before, the form factors $F_{1,2}^{(p+a)}$ are calculated for $\mu \to 0$ and decomposed in powers of Q^2, whereas $B_{1-3}^{(p+a)}$ are exact in this sense.

The zero-mode contribution $\Gamma_\rho^{(\mathrm{zm})}$ is calculated in Appendix D, Sec. D 3. The expression for $\Gamma_\rho^{(\mathrm{zm})}$ is given by Eq. (D21). We represent it in the form of decomposition (56). Then the form factors in this decomposition have the form

$$F_1^{(\mathrm{zm})} = 0, \tag{75a}$$

$$F_2^{(\mathrm{zm})} = 0, \tag{75b}$$

$$B_1^{(\mathrm{zm})} = -\frac{g^2}{16\pi^2}\log\frac{\Lambda_\perp}{m} + \frac{g^2}{16\pi^2}\varphi(Q^2), \tag{75c}$$

$$B_2^{(\mathrm{zm})} = \frac{g^2}{8\pi^2}\log\frac{\Lambda_\perp}{m} + \frac{g^2}{8\pi^2}\varphi(Q^2), \tag{75d}$$

$$B_3^{(\mathrm{zm})} = \frac{g^2}{32\pi^2 m^2}(6m^2 - 4\mu^2 + Q^2)\log\frac{\Lambda_\perp}{m} + \frac{g^2}{32\pi^2} - \frac{g^2}{32\pi^2 m^2}\left\{\mu^2\left(2\log\frac{m}{\mu} + 1\right) - (4m^2 - 2\mu^2 + Q^2)\varphi(Q^2)\right\}. \tag{75e}$$

The final expressions for the form factors are given by the sum of the corresponding quantities from Eqs. (74) and (75):

$$F_1 = \frac{g^2}{16\pi^2}\log\frac{\Lambda_\perp}{m} + \frac{g^2}{4\pi^2}\left(\log\frac{m}{\mu} - \frac{7}{8}\right) - \frac{g^2 Q^2}{24\pi^2 m^2}\left(\log\frac{m}{\mu} - \frac{9}{8}\right) + O(Q^4), \tag{76a}$$

$$F_2 = \frac{3g^2}{16\pi^2} - \frac{g^2 Q^2}{32\pi^2 m^2} + O(Q^4), \tag{76b}$$

$$B_1 = -\frac{g^2}{64\pi^2}, \tag{76c}$$

$$B_2 = -\frac{g^2}{32\pi^2}, \tag{76d}$$

$$B_3 = \frac{g^2}{32\pi^2}. \tag{76e}$$

The expressions for B_{1-3} are exact, i.e., these formulas are valid for any Q^2 and μ. That is, the Q^2-dependence coming from $B_{1-3}^{(p+a)}$, Eqs. (74c)–(74e), as well as the $\Lambda_\perp$-dependent terms are exactly canceled by the corresponding zero-mode contributions $B_{1-3}^{(zm)}$. The form factors $F_{1,2}$ and $B_{1,2}$ are the same as those obtained from the LFD diagrammatic approach, in Eqs. (61), while B_3's in Eqs. (61e) and (76e), are different. Moreover, B_{1-3} are not zeros, though we started from the Feynman expression for the EMV, which initially had no relation to the light front (i.e., to the four-vector ω). We will discuss this situation in more detail below, in Sec. IV.

2. Invariant regularization

To complete our analysis, we give here the form factors obtained from Eq. (69) by using an invariant regularization of the divergent integral over d^4k. The standard recipe consists in using the Feynman parametrization, then making the Wick rotation and imposing a cutoff Λ^2 on the modulus of the Euclidean four-momentum squared, similarly to how it has been done in Sec. II B 2. After that, identifying the structure of the EMV (69) with the decomposition (36), we reproduce the well-known result:[3]

$$F_1 = \frac{g^2}{32\pi^2}\log\frac{\Lambda^2}{m^2} + \frac{g^2}{4\pi^2}\left(\log\frac{m}{\mu} - \frac{15}{16}\right) - \frac{g^2 Q^2}{24\pi^2 m^2}\left(\log\frac{m}{\mu} - \frac{9}{8}\right) + O(Q^4), \tag{77a}$$

$$F_2 = \frac{3g^2}{16\pi^2} - \frac{g^2 Q^2}{32\pi^2 m^2} + O(Q^4). \tag{77b}$$

Equation (77b) exactly coincides with Eq. (76b) obtained for the rotationally noninvariant cutoffs. The formulas (76a) and (77a) differ by a constant (i.e., Q^2-independent) part. The corresponding form factors F_1^{ren} however also coincide after the renormalization (37).

In principle, one might identify the structure of the Feynman EMV (regularized by means of an invariant cutoff) with the LF decomposition (56) containing five form factors. In this case the formulas (77) would be found for $F_{1,2}$, while one would arrive at the evident result $B_{1-3} = 0$ for the other form factors.

The regularization of the EMV (69) by means of one PV boson results in the same formulas (77), changing Λ^2 to μ_1^2.

IV. DISCUSSION

We have shown above that the perturbative spin-1/2 fermion self-energy and the EMV calculated in LFD depend on the orientation of the LF plane, when the tradi-

[3] $F_2(Q^2 = 0)$ is an anomalous magnetic moment. Introducing the coupling constant $\alpha = g^2/(4\pi)$, we get in the Yukawa model $F_2(0) = 3\alpha/(4\pi)$, which differs by a factor of $3/2$ from the QED value $\alpha/(2\pi)$.

tional regularization in terms of the transverse and longitudinal cutoffs is applied to the corresponding amplitudes. This dependence reveals itself in the appearance of extra spin structures in the decompositions of the self-energy and the EMV in invariant amplitudes. In covariant LFD on the plane $\omega\cdot x = 0$ with $\omega^2 = 0$, it is conveniently parametrized through the four-vector ω. The corresponding decompositions for the self-energy and the EMV are given by Eqs. (7) and (56), respectively. The structure of the LF self-energy is characterized by the three scalar functions $\mathcal{A}$, $\mathcal{B}$, and $\tilde{C} = \mathcal{C}(p^2) + C_{fc}$, instead of the two usual ones, while the on-energy-shell EMV contains five form factors, the two standard $F_{1,2}$ and the three extra, B_{1-3}, ones.

Performing calculations of the self-energy by integrating the Feynman amplitude written in terms of the LF variables with the same cutoffs as in LFD, we did not encounter any ω-dependence in the final result, Eq. (29). The latter therefore does not coincide with the LFD self-energy (7). For the EMV, both methods lead to ω-dependent structures with five form factors. However, the EMV calculation by means of the LFD rules results in the set of form factors (61), whereas the calculation of the Feynman amplitude in terms of the LF variables gives a different set of form factors (76). Though this difference concerns the form factor B_3 only, the corresponding EMV's do not coincide nevertheless with each other.

The extra form factors do not, of course, appear when the Feynman amplitude is calculated with a spherically symmetric cutoff in four-dimensional space. This can be achieved, e.g., by imposing a direct cutoff on the Wick rotated integration variable in Euclidean space $|k^2| = \mathbf{k}^2 + k_4^2 < \Lambda^2$ or by using the PV regularization. In the case of LFD, we deal with three-dimensional integration variables. Therefore, constructing rotationally invariant (i.e., ω-independent) cutoffs which restrict a three-dimensional integration domain encounters serious difficulties since the integration domains in LFD amplitudes differ from each other, and it is not easy to restrict them simultaneously in a self-consistent way. This is a reason why the PV regularization looks much more preferable. It is naturally generalized to LFD and allows us to remove ultraviolet divergencies in an ω-independent way. We showed that in order to cancel completely all ω-dependent terms in the LF self-energy and the EMV it is necessary to use the PV subtractions for both the boson and fermion propagators. Note that this cancellation occurs for arbitrary (finite) PV masses. Simultaneously, all ultraviolet divergencies disappear. After that, the regularized LFD results coincide exactly with the Feynman ones calculated with the same PV subtractions.

The physical quantities, like the functions $\mathcal{A}$ and $\mathcal{B}$ in the self-energy or the form factors $F_{1,2}$ in the EMV, can be easily extracted from the corresponding amplitudes. Once we know the self-energy $\Sigma(p)$ explicitly, taking the traces

$$\mathrm{Tr}\{\Sigma(p)\} = 4g^2\mathcal{A}(p^2),$$
$$\mathrm{Tr}\{\Sigma(p)\not\omega\} = \frac{4g^2(\omega\cdot p)}{m}\mathcal{B}(p^2)$$

allows one to get $\mathcal{A}(p^2)$ and $\mathcal{B}(p^2)$, because the term $\sim\not\omega$ in the self-energy (7) does not contribute to these traces. To separate the physical electromagnetic form factors $F_{1,2}$ from the nonphysical ones, B_{1-3}, it is enough to consider the plus-component of the current (or, in terms of covariant LFD, the contraction of the current with ω_ρ) written in the form (56). Indeed, in the limit $\omega\cdot p = \omega\cdot p'$,

$$\bar{u}'\Gamma_+ u \equiv \bar{u}'(\omega\cdot\Gamma)u = \bar{u}'\left[F_1\not\omega + \frac{iF_2}{2m}\sigma_{\rho\nu}\omega_\rho q_\nu\right]u.$$

As we see, B_{1-3} dropped out from here. This is however not always the case since the decomposition (56) is not unique. Take, for instance, the decomposition of the same EMV given in Ref. [20]:

$$\bar{u}'\Gamma_\rho u = \bar{u}'\left\{\tilde{F}_1\gamma_\rho + \frac{i\tilde{F}_2}{2m}\sigma_{\rho\nu}q_\nu + B_1\left[\frac{\not\omega}{\omega\cdot p} - \frac{1}{m(1+\eta)}\right]\times(p+p')_\rho + B_2\frac{m\omega_\rho}{\omega\cdot p} + B_3\frac{m^2\not\omega\omega_\rho}{(\omega\cdot p)^2}\right\}u, \quad (78)$$

where $\eta = Q^2/4m^2$. It is easy to see that the form factors B_{1-3} in Eqs. (56) and (78) are identical, while

$$\tilde{F}_1 = F_1 - \frac{2\eta B_1}{1+\eta}, \qquad \tilde{F}_2 = F_2 - \frac{2B_1}{1+\eta}.$$

If we now identify $\tilde{F}_{1,2}$ with the physical form factors, they will differ from $F_{1,2}$, unless $B_1 = 0$. If we used for the regularization the LF cutoffs $\Lambda_\perp$ and ϵ, we would get $B_1 = -g^2/64\pi^2$ [see Eqs. (61c) and (76c)] and

$$\tilde{F}_1 = \frac{g^2}{16\pi^2}\log\frac{\Lambda_\perp}{m} + \frac{g^2}{4\pi^2}\left(\log\frac{m}{\mu} - \frac{7}{8}\right) - \frac{g^2Q^2}{24\pi^2m^2}\left(\log\frac{m}{\mu} - \frac{21}{16}\right) + O(Q^4),$$
$$\tilde{F}_2 = \frac{7g^2}{32\pi^2} - \frac{5g^2Q^2}{128\pi^2m^2} + O(Q^4).$$

$\tilde{F}_{1,2}$ do not coincide either with the Feynman form factors, given by Eqs. (77) (if we identify $\Lambda_\perp$ with Λ), or with the LFD ones defined by Eqs. (76a) and (76b). The regularization by the PV boson kills B_1 and this ambiguity disappears. However, if the nonphysical form factors are not canceled completely, the result is sensitive to the form of the EMV representation.

Although one can use the plus-component of the current (56) to extract the physical form factors in hadron phenomenology, it is not enough in many other cases, when the knowledge of the full matrix structure of the vertex is needed. For example, this occurs in LFD nonperturbative approaches, when the EMV enters as an off-energy-shell subgraph into a more complicated diagram. In such a case, one cannot simply ignore the extra spin structures, because they may contribute to observable quantities. The latter statement concerns the self-energy as well.

As our results show, the dependence on the LF plane orientation appears not only in LFD amplitudes, but also in Feynman ones, if we put the cutoffs in the LF variables $\mathbf{k}_\perp^2$ and x, i.e., constrain the integration domain by a spherically nonsymmetric region, the orientation of which follows the orientation of the LF plane. At first glance, this seems contradictory: (i) the extra form factors B_{1-3} [Eqs. (76c)–(76e)] originate from the spherically nonsymmetric cutoffs, but (ii) they do not depend on the cutoff values. This is in fact a normal situation which can be illustrated by the following toy example. Consider the three-dimensional integral:

$$I_{ij} = \int \frac{k_i k_j d^3k}{(\mathbf{k}^2 + m^2 + Q^2)^{5/2}} \equiv F_1 \delta_{ij}. \quad (79)$$

It is logarithmically divergent at infinity: $F_1 \sim \int d|\mathbf{k}|/|\mathbf{k}|$. Let us introduce the spherically symmetric cutoff $|\mathbf{k}| < L$. A simple calculation gives

$$F_1 = \frac{2\pi}{3} \log\frac{L^2}{m^2 + Q^2} + \frac{4\pi}{9}(\log 8 - 4) + O\left(\frac{1}{L}\right).$$

Let us now regularize this integral by a cutoff imposed on the two-dimensional variable $\mathbf{k}_\perp$ in the plane orthogonal to an arbitrary direction $\mathbf{n}$. That is, we set $\mathbf{k}_\perp^2 = \mathbf{k}^2 - (\mathbf{k} \cdot \mathbf{n})^2 < \Lambda_\perp^2$. In other words, we integrate over the volume of a cylinder of the radius $\Lambda_\perp$ and of infinite length, with the axis directed along $\mathbf{n}$. The initial integral turns into

$$I_{ij}^{\rm reg} = \int \frac{k_i k_j}{(\mathbf{k}^2 + m^2 + Q^2)^{5/2}} \theta[\Lambda_\perp^2 - \mathbf{k}^2 + (\mathbf{k}\cdot\mathbf{n})^2] d^3k$$
$$\equiv \tilde{F}_1 \delta_{ij} + B_1(\delta_{ij} - n_i n_j). \quad (80)$$

The integral along $\mathbf{n}$ (or over dk_z, if $\mathbf{n}$ is parallel to z) converges, similarly to the convergence of the integral over dx in the Feynman amplitude written through the LF variables. We see that the spherically nonsymmetric cutoff $\Lambda_\perp$ generates one extra form factor B_1, like this happens for the Feynman amplitude. We obtain

$$\tilde{F}_1 = \frac{2\pi}{3} \log\frac{\Lambda_\perp^2}{m^2 + Q^2} + O\left(\frac{1}{\Lambda_\perp}\right),$$
$$B_1 = -\frac{2\pi}{3} + O\left(\frac{1}{\Lambda_\perp}\right).$$

The leading terms $\propto \log L$ in F_1 and $\tilde{F}_1$ coincide, provided we identify $\Lambda_\perp$ with L. However, there is a difference in the finite parts: $F_1 - \tilde{F}_1 = \frac{4\pi}{9}(\log 8 - 4)$, like the difference between the term $\frac{15}{16}$ in Eq. (77a) and $\frac{7}{8}$ in Eq. (76a). The transverse cutoff $\Lambda_\perp$ generates a finite extra form factor B_1, which itself does not depend on $\Lambda_\perp$, similarly to B_{1-3} in the EMV. This example clearly mimics the properties of the above calculation of the electromagnetic form factors from the Feynman amplitude regularized by the LF cutoffs.

It is therefore misleading to think that one can derive some "true" LF amplitude starting with the covariant Feynman amplitude and calculating it in the LF variables: $I = \int \ldots d^4k = \int \ldots d^2k_\perp dx dk_-$. This integral diverges (except for some particular cases) and it has no sense without regularization. It depends on the size, shape, and orientation of the integration domain constrained by the regularization procedure. In other words, there is no "covariant Feynman amplitude" in itself. There exists only an inseparable couple: the covariant Feynman amplitude together with the rules to regularize it.

When we calculate amplitudes by means of the LFD graph technique rules, the noninvariant integration domain is not the only source of the ω-dependence. Another source is hidden in the rules themselves. Indeed, these rules are not obliged to reproduce exactly the amplitude which follows from the Feynman approach, even for the same integration domain D. The divergent (and, after regularization, cutoff-dependent) terms are treated nonidentically in the two approaches and may be different. This fact is illustrated by the above calculation of the form factor B_3 [cf. Eq. (61e) obtained within LFD with Eq. (76e) coming from the Feynman approach]. The renormalization procedures may be different too. However, the renormalized, observed amplitudes must be the same.

When the ω-dependent contributions to the self-energy and EMV survive, one has to cancel them with appropriate extra counterterms in the interaction Hamiltonian. These counterterms are inherent to the LFD Hamiltonian and should not be confused with the traditional charge and mass counterterms in the original Lagrangian. The need for such a counterterm for the renormalization of the self-energy was already advocated in Ref. [7], where the nonperturbative fermion mass renormalization was studied in the two-body approximation within covariant LFD. This new counterterm cancels the contribution $\sim \not\omega$ in the self-energy (7).

However, the introduction of additional specific counterterms may help only if their number is finite and tractable. For the case of the fermion self-energy we would need only one ω-dependent counterterm, since the coefficient $\tilde{C}$ is a constant. In the case of LFD calculations of the EMV, the form factor B_3 depends nontrivially on the momenta (through Q^2 and α), which would generate an infinite number of local counterterms to kill it, even in perturbation theory. For this reason, the use of counterterms cannot serve as a universal tool for the calculation of renormalized quantities in LFD with the traditional transverse and longitudinal cutoffs.

If the renormalization is done correctly, the dependence of any renormalized amplitude on the cutoffs disappears and the final result is the same, regardless of the type of the regularization used. However, from the practical point of view, the difficulty of calculations rapidly increases with introducing extra counterterms. Therefore, rotationally invariant regularization (like the PV one) seems by far more preferable in the LFD framework. The approach developed in Ref. [21], regularizing field theory by defining fields as distributions, could provide another method of rotationally invariant regularization.

V. CONCLUSION

We have calculated perturbatively the fermion self-energy and the EMV in the Yukawa model, in two different ways: (i) by the LFD graph technique rules, taking into account all necessary diagrams; (ii) by integrating the Feynman amplitudes in terms of the LF variables (i.e., the transverse and longitudinal parts of momenta) and summing up the pole, arc, and zero-mode contributions. For the same set of the cutoffs imposed on the LF variables, both methods give different results for the regularized amplitudes. This difference disappears if the invariant PV regularization is used instead of the rotationally noninvariant one.

Such properties follow from the fact that the cutoffs constrain a spherically nonsymmetrical integration domain, the symmetry being destroyed by the choice of a distinguished direction defined by the orientation of the LF surface. The dependence of regularized amplitudes on the LF plane orientation is conveniently taken into account in the explicitly covariant version of LFD by constructing extra spin structures. To exclude these structures from the physically observed quantities, one may introduce new counterterms in the interaction Hamiltonian, which also depend on the LF plane orientation. Taking them into account, one can calculate the renormalized amplitudes.

The use of spherically symmetric (in four-dimensional space) regularization, like, for instance, the PV one, considerably simplifies calculations. In perturbation theory it allows one to avoid the presence of these extra counterterms at all.

ACKNOWLEDGMENTS

Two of us (V. A. K. and A. V. S.) are sincerely grateful for the warm hospitality of the Laboratoire de Physique Corpusculaire, Université Blaise Pascal, in Clermont-Ferrand, where the present study was performed. This work has been partially supported by the RFBR Grant No. 05-02-17482-a.

APPENDIX A: KINEMATICAL RELATIONS

We give below some kinematical relations used in the self-energy and EMV calculations within covariant LFD. Amplitudes of the LF diagrams are expressed through the three-dimensional integrals over $d^3k/\varepsilon_{\mathbf{k}}$. Take the four-vectors $k = (\varepsilon_{\mathbf{k}}, \mathbf{k})$ and $p = (p_0, \mathbf{p})$, and construct a new four-vector $R = k - xp$ with $x = (\omega \cdot k)/(\omega \cdot p)$. Since $\omega \cdot R = 0$ and $\omega^2 = 0$, in the reference frame, where $\mathbf{p} = \mathbf{0}$, we have $\varepsilon_{\mathbf{k}} - xp_0 - |\mathbf{k}_\parallel| = 0$. Taking into account that $\varepsilon_{\mathbf{k}} = \sqrt{\mathbf{k}_\perp^2 + \mathbf{k}_\parallel^2 + \mu^2}$ and changing p_0 to $\sqrt{p^2}$, we arrive at the relations

$$|\mathbf{k}_\parallel| = \frac{\mathbf{k}_\perp^2 + \mu^2 - x^2p^2}{2x\sqrt{p^2}}, \qquad \varepsilon_{\mathbf{k}} = \frac{\mathbf{k}_\perp^2 + \mu^2 + x^2p^2}{2x\sqrt{p^2}}.$$

In the variables $\mathbf{k}_\perp$ and x, the invariant phase space element becomes

$$d^3k/\varepsilon_{\mathbf{k}} = d^2k_\perp dx/x. \tag{A1}$$

We can now express the scalar product $k \cdot p$ entering the quantity τ, Eq. (4), through $\mathbf{k}_\perp^2$ and x. For this purpose, we represent the invariant quantity R^2 in two different ways:

$$R^2 = (k - xp)^2 = \mu^2 - 2x(k \cdot p) + x^2p^2$$

and

$$R^2 = (\varepsilon_{\mathbf{k}} - xp_0)^2 - \mathbf{k}_\perp^2 - \mathbf{k}_\parallel^2 = -\mathbf{k}_\perp^2.$$

Equating the right-hand sides of these expressions yields

$$k \cdot p = \frac{\mathbf{k}_\perp^2 + \mu^2 + x^2p^2}{2x}. \tag{A2}$$

In the calculation of the EMV we have one more four-vector p'. We define two new four-vectors $R = k - xp$ and $R' = k - x'p'$, where $x' = (\omega \cdot k)/(\omega \cdot p') = x/(1 + \alpha)$. From the equalities $\omega \cdot R = \omega \cdot R' = 0$, in the reference frame, where $\mathbf{p} = \mathbf{0}$, follows $R^2 = -\mathbf{R}_\perp^2 = -\mathbf{k}_\perp^2$, $R'^2 = -\mathbf{R}_\perp'^2 = -(\mathbf{k}_\perp - x'\mathbf{\Delta})^2$, where $\mathbf{\Delta} = \mathbf{p}'_\perp = \mathbf{q}_\perp$. Analogously to Eq. (A2), we get from here

$$k \cdot p = \frac{\mathbf{k}_\perp^2 + \mu^2 + x^2m^2}{2x}, \tag{A3a}$$

$$k \cdot p' = \frac{(\mathbf{k}_\perp - x'\mathbf{\Delta})^2 + \mu^2 + x'^2m^2}{2x'}. \tag{A3b}$$

From these formulas follow the expressions (45a) and (45b). For completeness, we give here the other scalar products which are needed for the EMV calculations:

$$\omega \cdot k = x(\omega \cdot p), \qquad \omega \cdot p' = (1 + \alpha)(\omega \cdot p),$$
$$p \cdot p' = \frac{Q^2}{2} + m^2, \qquad \omega^2 = 0,$$
$$p^2 = p'^2 = m^2, \qquad k^2 = \mu^2.$$

After integrating over the azimuthal angle of the vector $\mathbf{k}_\perp$, the form factors depend on $\mathbf{\Delta}^2$, and one should relate it with the invariant square of the momentum transfer $Q^2 = -(p' - p)^2$. If one had $\omega \cdot p = \omega \cdot p'$ (equivalent to $\alpha = 0$), it would be simply $Q^2 = \mathbf{\Delta}^2$. In our case the relation is more complicated. Indeed, since $\omega \cdot p = \omega_0 m$, we have, on the one hand, $\omega \cdot p' = (1 + \alpha)\omega_0 m$, and, on the other hand, $\omega \cdot p' = \omega_0(\sqrt{\mathbf{\Delta}^2 + \mathbf{p}_\parallel'^2 + m^2} - |\mathbf{p}'_\parallel|)$. We thus find

$$|\mathbf{p}'_{\|}| = \frac{\mathbf{\Delta}^2 - m^2\alpha(2+\alpha)}{2m(1+\alpha)}$$

and

$$Q^2 = (\sqrt{\mathbf{\Delta}^2 + \mathbf{p}'^2_{\|} + m^2} - m)^2 - \mathbf{\Delta}^2 - \mathbf{p}'^2_{\|} = \frac{\mathbf{\Delta}^2 + \alpha^2 m^2}{1+\alpha}. \quad \text{(A4)}$$

From here Eq. (46) follows.

APPENDIX B: DERIVING THE LIGHT-FRONT SELF-ENERGY FROM THE FEYNMAN APPROACH

Proceeding from the Feynman amplitude (19) for the self-energy, Sec. II B, we calculate here the pole, arc, and zero-mode contributions.

1. Pole and arc contributions

We first consider the integral over dk_- in Eq. (20) for the x-integration in the limits $-\infty < x < -\epsilon$, $\epsilon < x < 1-\epsilon$, and $1+\epsilon < x < +\infty$, determining $\Sigma_{p+a}(p)$. It can be calculated directly (by primitive). However, in order to get the results in a form closer to LFD, we will use the residues. The integrand has two poles in the points

$$k_- = k_-^{(1)} \equiv \frac{\mathbf{k}_\perp^2 + \mu^2 - i0}{xp_+}$$

and

$$k_- = k_-^{(2)} \equiv p_- - \frac{\mathbf{k}_\perp^2 + m^2 - i0}{(1-x)p_+}.$$

If $-\infty < x < -\epsilon$ or $1+\epsilon < x < +\infty$, both poles lay, respectively, above or below the real axis. If $\epsilon < x < 1-\epsilon$ the poles are situated on the opposite sides from the real axis. We close the integration contour by an arc of a circle of the radius L, either in the upper half-plane or in the lower one, so that the pole $k_-^{(2)}$ is always outside the contour. The situation is illustrated in Fig. 6, where the integration contour is shown for the case $\epsilon < x < 1-\epsilon$.

Note that the order of integrations we have chosen in Eq. (20) requires some care in treating the cutoffs. Since the integration over dk_- is performed first, we should keep L arbitrary large, while the other cutoffs ϵ and $\Lambda_\perp$ are considered as being finite. In other words, we imply that $L \gg \Lambda_\perp^2/(m\epsilon)$. Such a convention ensures mutual position of the poles and the contour, as exposed above. Then $\Sigma_{p+a}(p)$ is represented as

$$\Sigma_{p+a}(p) = \frac{ig^2 p_+}{32\pi^4} \int d^2k_\perp \left[\int_\epsilon^{1-\epsilon} (\Sigma_{\text{pole}} - \Sigma_{\text{arc,low}}) dx - \int_{-\infty}^{-\epsilon} \Sigma_{\text{arc,low}} dx - \int_{1+\epsilon}^{+\infty} \Sigma_{\text{arc,up}} dx \right], \quad \text{(B1)}$$

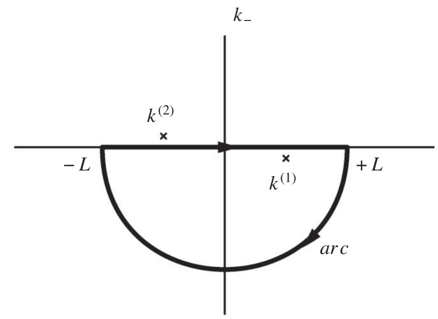

FIG. 6. Contour of the integration over dk_-. Positions of the poles are shown for $\epsilon < x < 1-\epsilon$.

where Σ_{pole} is the residue at the pole $k_-^{(1)}$, multiplied by $-2\pi i$, while $\Sigma_{\text{arc,low}}$ and $\Sigma_{\text{arc,up}}$ come from the integrations along the arcs in the lower and upper half-planes, respectively. The result for Σ_{pole} reads

$$\Sigma_{\text{pole}} = \frac{2\pi i(\not{p} - \not{k} + m)}{p_+[\mathbf{k}_\perp^2 + m^2 x - p^2 x(1-x) + \mu^2(1-x)]}. \quad \text{(B2)}$$

The four-vector k here is an on-mass-shell four-vector ($k^2 = \mu^2$) with the components expressed through $\mathbf{k}_\perp$ and x as follows: $k \equiv (k_-, k_+, \mathbf{k}_\perp) = (\frac{\mathbf{k}_\perp^2 + \mu^2}{xp_+}, xp_+, \mathbf{k}_\perp)$. To calculate $\Sigma_{\text{arc,low}}$ and $\Sigma_{\text{arc,up}}$, we should move along the arc in the clockwise and counterclockwise directions, respectively. In the points of the arc $k_- = Le^{i\phi}$ and $dk_- = iLe^{i\phi}d\phi$, where ϕ is an azimuthal angle. In the limit $L \to \infty$, we retain in the integrand the dominating k_--term. We thus obtain

$$\Sigma_{\text{arc,low}} = -\Sigma_{\text{arc,up}} = -\frac{\pi i}{2p_+^2} \frac{\gamma_+}{x(1-x)}. \quad \text{(B3)}$$

Substituting Eqs. (B2) and (B3) into Eq. (B1) and going over to the explicitly covariant notations by means of the identities $\gamma_+ = \not{\omega}$, $p_+ = \omega \cdot p$, we obtain that $\Sigma_{p+a}(p)$ is given by Eq. (23).

2. Zero modes

Consider now the zero-mode term $\Sigma_{\text{zm}}(p)$. We denote

$$\Sigma_{\text{zm}}(p) \equiv \Sigma_{\text{zm}}^{(0)}(p) + \Sigma_{\text{zm}}^{(1)}(p),$$

where the two items on the right-hand side correspond to the contributions to Eq. (20) from the infinitesimal integration regions $-\epsilon < x < \epsilon$ and $1-\epsilon < x < 1+\epsilon$, respectively. Take first $\Sigma_{\text{zm}}^{(0)}(p)$ (bosonic zero modes). If $x = 0$, the term $k_- p_+ x$ in the denominator of the integrand disappears and the integral over dk_- diverges linearly. This infinite contribution should therefore be proportional to $\delta(x)$. We take $x \to 0$ and keep in the numerator and in the denominator of the integrand in Eq. (20) the leading k_--terms (where k_- is not multiplied by x) only. That is

$$\Sigma^{(0)}_{\rm zm} = \frac{ig^2 p_+}{32\pi^4}\int d^2k_\perp \int_{-\epsilon}^{\epsilon} dx \int_{-L}^{L} dk_- \times \frac{1}{[k_- p_+ x - \mathbf{k}_\perp^2 - \mu^2 + i0]} \frac{-\frac{1}{2}\gamma_+ k_-}{(-k_- p_+)}. \quad \text{(B4)}$$

The double integral over $dxdk_-$ is of the type of Eq. (E1) with $b = (\mathbf{k}_\perp^2 + \mu^2)/p_+$ and $h = 0$ (see Appendix E). Using Eq. (E2), we obtain, in the covariant notations:

$$\Sigma^{(0)}_{\rm zm}(p) = \frac{g^2 \not\omega}{32\pi^3(\omega\cdot p)}\int d^2k_\perp \left[\log\frac{(\omega\cdot p)L}{\mathbf{k}_\perp^2 + \mu^2} - \log\frac{1}{\epsilon} - \frac{i\pi}{2}\right]. \quad \text{(B5)}$$

Changing the variable $x \to 1 - x$, for $\Sigma^{(1)}_{\rm zm}(p)$ (fermionic zero modes) we similarly get

$$\Sigma^{(1)}_{\rm zm}(p) = \frac{g^2 \not\omega}{32\pi^3(\omega\cdot p)}\int d^2k_\perp \left[\log\frac{(\omega\cdot p)L}{\mathbf{k}_\perp^2 + m^2} - \log\frac{1}{\epsilon} - \frac{i\pi}{2}\right]. \quad \text{(B6)}$$

Taking the sum of (B5) and (B6), we find that it has the form of Eq. (26): $\Sigma_{\rm zm}(p) \equiv g^2 C_{\rm zm}\frac{m\not\omega}{\omega\cdot p}$ with

$$C_{\rm zm} = \frac{g^2}{32\pi^2}\int_0^{\Lambda_\perp^2} d\mathbf{k}_\perp^2 \log\frac{\mathbf{k}_\perp^2 + m^2}{\mathbf{k}_\perp^2 + \mu^2}.$$

Calculating this integral, we find Eq. (27) for $C_{\rm zm}$.

APPENDIX C: LIGHT-FRONT CONTRIBUTIONS TO THE FORM FACTORS

In this Appendix, starting with the LF vertices $\Gamma_\rho^{(A)}$, $\Gamma_\rho^{(B)}$, and $\Gamma_\rho^{(C)}$ found in Sec. III A 2, Eqs. (52a)–(52c), we calculate their contributions to form factors $F_{1,2}$, B_{1-3}.

1. Preliminary transformations

Each contribution to a form factor $\mathcal{F}$ ($\mathcal{F} \equiv F_i$ or B_i) from the vertices $\Gamma_\rho^{(A)}$, $\Gamma_\rho^{(B)}$, or $\Gamma_\rho^{(C)}$ can be written as an integral of the form

$$\mathcal{F} = \int_{x_{\rm min}}^{x_{\rm max}} dx \int_0^{\Lambda_\perp^2} d\mathbf{k}_\perp^2 \int_0^{2\pi} d\phi f(\mathbf{k}_\perp^2, x, \phi, Q^2, \alpha), \quad \text{(C1)}$$

where ϕ is the angle between the two-dimensional vectors $\mathbf{k}_\perp$ and $\mathbf{\Delta}$, f is a given function (f's are different for different form factors), and the modulus of $\mathbf{\Delta}$ is expressed through Q^2 by Eq. (46). The limits $x_{\rm min}$ and $x_{\rm max}$ depend on which vertex is considered.

The analysis of the dependence of the form factors on the cutoff $\Lambda_\perp$ (when it tends to infinity) allows one to represent each of them as

$$\mathcal{F} = a_1\Lambda_\perp^2 + a_2\log\frac{\Lambda_\perp}{m} + a_{\rm reg}, \quad \text{(C2)}$$

where the coefficients a_1, a_2, and $a_{\rm reg}$ are regular functions depending on the particle masses, Q^2, and α, but independent of $\Lambda_\perp$. If $\alpha \neq 0$, no other divergencies (i.e., cutoff-dependent terms) excepting those listed in Eq. (C2) appear. Since the coefficients a_1 and a_2 determine the dependence of the form factors on the cutoff, we will calculate them at arbitrary α, in order to see in detail how the cutoff disappears (if so) after taking into account all the contributions $\Gamma_\rho^{(A)}$, $\Gamma_\rho^{(B)}$, and $\Gamma_\rho^{(C)}$ to the full EMV and its subsequent renormalization. As far as the coefficients $a_{\rm reg}$ are concerned, we will find them in the limit $\alpha \to 0$, retaining nonvanishing terms only. This simplifies calculations a lot, but leads to the same final result as if α was nonzero.

Although direct integrations over $d\phi$ and $d\mathbf{k}_\perp^2$ can always be done analytically for arbitrary Q^2 and α, the results turn out to be very cumbersome, so that the final integration over dx (if it can be done analytically) takes too much time. To make the computations more effective, we will proceed in the following way. We take the initial expression for a given form factor in the form of Eq. (C1) and study the behavior of the integrand as a function of $\mathbf{k}_\perp^2$ in the asymptotic region $|\mathbf{k}_\perp| \to \infty$. For this purpose we decompose it in a Laurent series:

$$f(\mathbf{k}_\perp^2, x, \phi, Q^2, \alpha) = f_0(x, Q^2, \alpha) + \frac{f_1(x, Q^2, \alpha)\cos\phi}{|\mathbf{k}_\perp|} + \frac{f_2(x, \phi, Q^2, \alpha)}{\mathbf{k}_\perp^2} + \cdots. \quad \text{(C3)}$$

We use this decomposition in order to define the functions f_0 and f_2 (the term with f_1 drops out after the integration over $d\phi$). We then represent f as a sum

$$f(\mathbf{k}_\perp^2, x, \phi, Q^2, \alpha) \equiv f_{\rm reg}(\mathbf{k}_\perp^2, x, \phi, Q^2, \alpha) + f_0(x, Q^2, \alpha) + \frac{\Phi_2(x, Q^2, \alpha)}{\mathbf{k}_\perp^2 + m^2\beta(x)}, \quad \text{(C4)}$$

where

$$\Phi_2(x, Q^2, \alpha) = \frac{1}{2\pi}\int_0^{2\pi} f_2(x, \phi, Q^2, \alpha)d\phi \quad \text{(C5)}$$

and $\beta(x)$ is a positive function which can be chosen in any convenient way in order to avoid the singularity at $\mathbf{k}_\perp^2 \to 0$. Equation (C4) should be considered as a definition of the function $f_{\rm reg}(\mathbf{k}_\perp^2, x, \phi, Q^2, \alpha)$. The latter, after the integration over $d\phi$, decreases faster than $1/\mathbf{k}_\perp^2$ in the asymptotic region, and its integration over $d\mathbf{k}_\perp^2$ does not require any regularization. The functions $f_0(x, Q^2, \alpha)$ and $\Phi_2(x, Q^2, \alpha)$ are rather simple, so that the two last addenda on the right-hand side of Eq. (C4) can be easily integrated over all the variables.

After separating out the terms which slowly decrease when $|\mathbf{k}_\perp| \to \infty$, we remain with a set of regular functions $f_{\rm reg}$. At arbitrary α, these functions are even more complicated than the initial integrands f. However, we calculate the regular contributions to the form factors in the limit $\alpha \to 0$. So, it is enough to consider the limiting functions $f_{\rm reg}(\mathbf{k}_\perp^2, x, \phi, Q^2, \alpha \to 0)$ which are much simpler than $f(\mathbf{k}_\perp^2, x, \phi, Q^2, \alpha)$. If $f_{\rm reg}$ is singular at $\alpha \to 0$, we decompose it in powers of α and retain all nonvanishing terms.

The trick exposed above allows one to find the coefficients in Eq. (C2). Indeed, substituting Eq. (C4) into Eq. (C1), we get

$$a_1 = 2\pi \int_{x_{\rm min}}^{x_{\rm max}} f_0(x, Q^2, \alpha)dx, \tag{C6a}$$

$$a_2 = 4\pi \int_{x_{\rm min}}^{x_{\rm max}} \Phi_2(x, Q^2, \alpha)dx, \tag{C6b}$$

$$a_{\rm reg} = \int_{x_{\rm min}}^{x_{\rm max}} dx \left\{ \left[\int_0^\infty d\mathbf{k}_\perp^2 \int_0^{2\pi} d\phi f_{\rm reg}(\mathbf{k}_\perp^2, x, \phi, Q^2, \alpha \to 0) \right] - 2\pi \Phi_2(x, Q^2, \alpha \to 0) \log\beta(x) \right\}. \tag{C6c}$$

The integrations over $d\phi$ and $d\mathbf{k}_\perp^2$ can be done analytically for all the five form factors. For $F_{1,2}$ the results of the remaining integrations over dx at arbitrary Q^2 and μ are not expressed through elementary functions. In order to simplify the formulas, we decompose both $F_{1,2}$ in powers of Q^2 up to terms of order Q^2 and take the limit $\mu \to 0$. Concerning the form factors B_{1-3}, all the integrations are performed analytically without any approximation.

Below, in Secs. C 2–C 4, we list the coefficients a_1, a_2, and $a_{\rm reg}$ entering Eq. (C2), pointing out in superscripts which form factor the given coefficient belongs to. The coefficients are calculated by means of Eqs. (C6), separately for the vertices $\Gamma_\rho^{(A)}$, $\Gamma_\rho^{(B)}$, and $\Gamma_\rho^{(C)}$ [see Eqs. (54) and (55)].

2. Contribution to the form factors from $\Gamma_\rho^{(A)}$

It is convenient to set in Eq. (C4) $\beta(x) = x^2 + \frac{\mu^2}{m^2} \times (1 - x)$. The limits of the x-integration are $x_{\rm min} = 0$, $x_{\rm max} = 1$. Then

$$a_1^{F_1} = a_1^{F_2} = a_1^{B_1} = a_1^{B_2} = a_1^{B_3} = 0, \tag{C7}$$

$$a_2^{F_1} = \frac{g^2[2(1+\alpha)Q^2 + \alpha^2(2-\alpha^2)m^2]}{16\pi^2(1+\alpha)^2 z_\alpha}, \qquad a_2^{F_2} = 0, \qquad a_2^{B_1} = \frac{g^2(2+\alpha)[(1+\alpha)Q^2 + \alpha^2 m^2]}{16\pi^2(1+\alpha)^2 z_\alpha},$$
$$a_2^{B_2} = \frac{g^2}{16\pi^2(1+\alpha)}\left\{\frac{4\alpha^2(2+2\alpha+\alpha^2)m^2 + [8+\alpha(2+\alpha)(8+2\alpha+\alpha^2)]Q^2}{(1+\alpha)(2+\alpha)z_\alpha} - 4\right\},$$
$$a_2^{B_3} = \frac{g^2}{16\pi^2 m^2(1+\alpha)^2}\left\{(2+\alpha)\mu^2 - \frac{(3+3\alpha+\alpha^2)m^2}{1+\alpha} - \frac{Q^2[(1+\alpha)Q^2 - \alpha^2 m^2]}{z_\alpha}\right\}, \tag{C8}$$

where $z_\alpha = (2 + 2\alpha + \alpha^2)Q^2 + 2\alpha^2 m^2$, and

$$a_{\rm reg}^{F_1} = \frac{g^2}{4\pi^2}\left(\log\frac{m}{\mu} - \frac{7}{8}\right) - \frac{g^2 Q^2}{24\pi^2 m^2}\left(\log\frac{m}{\mu} - \frac{9}{8}\right) + O(Q^4), \qquad a_{\rm reg}^{F_2} = \frac{3g^2}{16\pi^2} - \frac{g^2 Q^2}{32\pi^2 m^2} + O(Q^4),$$
$$a_{\rm reg}^{B_1} = \frac{g^2}{64\pi^2}[-1 + 4\varphi(Q^2)], \qquad a_{\rm reg}^{B_2} = -\frac{g^2}{32\pi^2}[1 + 4\varphi(Q^2)],$$
$$a_{\rm reg}^{B_3} = \frac{g^2}{32\pi^2 m^2}\left[\mu^2\left(2\log\frac{m}{\mu} + 1\right) - (4m^2 - 2\mu^2 + Q^2)\varphi(Q^2)\right], \tag{C9}$$

with

$$\varphi(Q^2) = 1 - \sqrt{1 + \frac{4m^2}{Q^2}} \log\left(\frac{\sqrt{Q^2 + 4m^2} + \sqrt{Q^2}}{2m}\right). \tag{C10}$$

3. Contribution to the form factors from $\Gamma_\rho^{(B)}$

We set $\beta(x) = 1$, $x_{\rm min} = 1$, $x_{\rm max} = 1 + \alpha$. We thus get

$$
\begin{aligned}
a_1^{F_1} &= a_1^{F_2} = a_1^{B_1} = a_1^{B_2} = 0,\\
a_1^{B_3} &= -\frac{g^2}{32\pi^2 m^2}\frac{\log(1+\alpha)}{\alpha(1+\alpha)},\\
a_2^{F_1} &= \frac{g^2}{16\pi^2}\left[1 - \frac{2(1+\alpha)Q^2 + \alpha^2(2-\alpha^2)m^2}{(1+\alpha)^2 z_\alpha}\right],\\
a_2^{F_2} &= 0,\\
a_2^{B_1} &= -\frac{g^2(2+\alpha)[(1+\alpha)Q^2 + \alpha^2 m^2]}{16\pi^2(1+\alpha)^2 z_\alpha},\\
a_2^{B_2} &= -\frac{g^2}{16\pi^2(1+\alpha)}\left\{\frac{4\alpha^2(2+2\alpha+\alpha^2)m^2 + [8+\alpha(2+\alpha)(8+2\alpha+\alpha^2)]Q^2}{(1+\alpha)(2+\alpha)z_\alpha} - 4\right\},\\
a_2^{B_3} &= -\frac{g^2}{16\pi^2 m^2(1+\alpha)^2}\left\{\mu^2 - \frac{(2+\alpha)m^2}{1+\alpha} - \frac{Q^2[(1+\alpha)Q^2 - \alpha^2 m^2]}{z_\alpha}\right\}.
\end{aligned}
\tag{C11}
$$

While integrating over dx in Eq. (C6c), we introduce a new variable $\xi = (x-1)/\alpha$. Then

$$
\int_1^{1+\alpha} dx(\cdots) = \alpha \int_0^1 d\xi(\cdots).
$$

After that the integrands $f_{\rm reg}$ should be decomposed in powers of α up to terms of order $1/\alpha$. Performing this transformation, we obtain the following result:

$$
\begin{aligned}
&a_{\rm reg}^{F_1} = a_{\rm reg}^{F_2} = 0, \qquad a_{\rm reg}^{B_1} = -\frac{1}{2}a_{\rm reg}^{B_2} = -\frac{g^2}{16\pi^2}\varphi(Q^2),\\
&a_{\rm reg}^{B_3} = \frac{g^2}{32\pi^2 m^2}\left[\frac{Q^2}{\alpha} + (4m^2 - 2\mu^2 + Q^2)\varphi(Q^2)\right]
\end{aligned}
\tag{C12}
$$

with $\varphi(Q^2)$ given by Eq. (C10).

4. Contribution to the form factors from $\Gamma_\rho^{(C)}$

The matrix structure of the vertex $\Gamma_\rho^{(C)}$ is the same as the one in front of the form factor B_3 in the decomposition (56). For this reason $\Gamma_\rho^{(C)}$ contributes to B_3 only. From Eq. (60) we easily find

$$
a_1^{B_3} = \frac{g^2}{32\pi^2 m^2}\frac{\log(1+\alpha)}{\alpha(1+\alpha)},
\tag{C13}
$$

all the other coefficients being zero.

APPENDIX D: DERIVING THE LIGHT-FRONT ELECTROMAGNETIC VERTEX FROM THE FEYNMAN APPROACH

Proceeding from the Feynman amplitude (69) for the EMV, Sec. III B, we calculate here the pole, arc, and zero-mode contributions.

1. Preliminary transformations

Under the condition $p'_+ - p_+ = 0$, the LF components of the four-vectors p and p' are

$$
\begin{aligned}
&\mathbf{p}_\perp = 0, \qquad p_- = \frac{m^2}{p_+}, \qquad \mathbf{p}'_\perp = \mathbf{q}_\perp,\\
&p'_- = \frac{\mathbf{q}_\perp^2 + m^2}{p_+},
\end{aligned}
\tag{D1}
$$

where $\mathbf{q}_\perp$ is the transversal part of the three-dimensional momentum transfer:

$$
\mathbf{q}_\perp = \mathbf{p}'_\perp - \mathbf{p}_\perp, \qquad Q^2 = -(p'-p)^2 = \mathbf{q}_\perp^2.
$$

Introducing a new variable x by means of the relation $k_+ = xp_+$ and using the notations

$$
\begin{aligned}
&a = \frac{\mathbf{k}_\perp^2 + \mu^2}{p_+}, \qquad b = \frac{\mathbf{k}_\perp^2 + m^2}{p_+},\\
&b' = \frac{(\mathbf{k}_\perp - \mathbf{q}_\perp)^2 + m^2}{p_+},
\end{aligned}
\tag{D2}
$$

we cast Eq. (70) in the form

$$
\Gamma_\rho = \frac{ig^2}{128\pi^4 p_+^2}\int d^2k_\perp \int_{-\infty}^{+\infty} dx \int_{-\infty}^{+\infty} \frac{dk_-[k_-\gamma_+ + \mathcal{M}']\gamma_\rho[k_-\gamma_+ + \mathcal{M}]}{v_1 v_2 v'_2},
\tag{D3}
$$

where

$$\begin{aligned} v_1 &= xk_- - a + i0, \\ v_2 &= (x-1)k_- - b - (x-1)p_- + i0, \\ v_2' &= (x-1)k_- - b' - (x-1)p'_- + i0, \end{aligned} \tag{D4}$$

$$\begin{aligned} \mathcal{M} &= (x-1)p_+\gamma_- - p_-\gamma_+ - 2\mathbf{k}_\perp \cdot \boldsymbol{\gamma}_\perp - 2m, \\ \mathcal{M}' &= (x-1)p_+\gamma_- - p'_-\gamma_+ - 2(\mathbf{k}_\perp - \mathbf{q}_\perp)\cdot \boldsymbol{\gamma}_\perp - 2m. \end{aligned} \tag{D5}$$

The matrices $\mathcal{M}$ and $\mathcal{M}'$ do not depend on k_-.

The integral in Eq. (D3) diverges at $|\mathbf{k}_\perp| \to \infty$. If $x = 0$ or $x = 1$, it diverges also at $k_- \to \pm\infty$. We constrain the integration over $d\mathbf{k}_\perp^2$ in $d^2k_\perp = \frac{1}{2} d\mathbf{k}_\perp^2 d\phi$ by the cutoff $\Lambda_\perp^2$, and introduce also the cutoffs L in k_-, as in Eq. (21), and ϵ in x, splitting the region of the integration over dx into three normal regions $-\infty < x < -\epsilon$, $\epsilon < x < 1-\epsilon$, $1+\epsilon < x < +\infty$, and two infinitesimal ones $-\epsilon < x < \epsilon$, $1-\epsilon < x < 1+\epsilon$. The integrals over the normal regions are calculated by summing up the residue and arc contributions, as in Sec. II B 1. The contributions (if any) from the two infinitesimal regions of the integration over dx, which do not vanish in the limit $\epsilon \to 0$, correspond to the zero modes. Because of rather weak (logarithmic) divergence of the initial integral (69), we expect that the result of the full integration over dk_- and dx has a finite limit at $L \to \infty$ and $\epsilon \to 0$, while the remaining integration over $d^2k_\perp$ produces logarithmic dependence of the EMV on the cutoff $\Lambda_\perp$.

2. Pole and arc contributions

We start with the calculation of $\Gamma_\rho^{(p+a)}$. The procedure is quite similar to that exposed in Appendix B 1 and in the papers [9,10,15–17]. The integrand in Eq. (D3) has three poles:

$$k_-^{(1)} = \frac{a - i0}{x}, \qquad k_-^{(2)} = \frac{b + (x-1)p_- - i0}{x-1}, \qquad k_-^{(3)} = \frac{b' + (x-1)p'_- - i0}{x-1}. \tag{D6}$$

If $-\infty < x < -\epsilon$ or $1+\epsilon < x < +\infty$, all of them are, respectively, either in the upper half-plane of k_- or in the lower one. If $\epsilon < x < 1-\epsilon$, the pole $k_-^{(1)}$ is in the lower half-plane, while the poles $k_-^{(2)}$ and $k_-^{(3)}$ are in the upper one. We can thus write, analogously to Eq. (B1):

$$\Gamma_\rho^{(p+a)} = \frac{ig^2}{128\pi^4 p_+^2} \int d^2k_\perp \bigg[\int_\epsilon^{1-\epsilon} (\Gamma_\rho^{\rm pole} - \Gamma_\rho^{\rm arc,low}) dx - \int_{-\infty}^{-\epsilon} \Gamma_\rho^{\rm arc,low} dx - \int_{1+\epsilon}^{+\infty} \Gamma_\rho^{\rm arc,up} dx \bigg], \tag{D7}$$

where $\Gamma_\rho^{\rm pole}$ equals the residue of the integrand in the pole $k_- = k_-^{(1)}$, multiplied by $-2\pi i$:

$$\Gamma_\rho^{\rm pole} = -\frac{8\pi i p_+^2}{x} \frac{(\not p' - \not k + m)\gamma_\rho(\not p - \not k + m)}{[(p'-k)^2 - m^2][(p-k)^2 - m^2]} \tag{D8}$$

with $k^2 = \mu^2$, and the arc contributions are

$$\Gamma_\rho^{\rm arc,low} = -\Gamma_\rho^{\rm arc,up} = -\frac{\pi i}{x(1-x)^2}\gamma_+\gamma_\rho\gamma_+. \tag{D9}$$

Substituting Eqs. (D8) and (D9) into Eq. (D7), we find

$$\Gamma_\rho^{(p+a)} = \frac{g^2}{16\pi^3}\int d^2k_\perp \bigg\{ \int_\epsilon^{1-\epsilon} \frac{dx}{x} \frac{(\not p' - \not k + m)\gamma_\rho(\not p - \not k + m)}{[(p'-k)^2 - m^2][(p-k)^2 - m^2]} - \frac{\gamma_+\gamma_\rho\gamma_+}{4p_+^2}\log\frac{1}{\epsilon}\bigg\}. \tag{D10}$$

We substitute here $\log(1/\epsilon)$ by $\int_\epsilon^1 dx/x$ and take the limit $\epsilon \to 0$. The latter is achieved simply by setting $\epsilon = 0$ in the integration limits, because the integrand is no more singular either at $x = 0$ or at $x = 1$. We also return to the covariant notations, replacing γ_+ by $\not\omega$ and p_+ by $\omega \cdot p$. In this way we find that $\Gamma_\rho^{(p+a)}$ is given by Eq. (72).

3. Zero modes

Let us now consider the zero-mode contribution to Eq. (D3). It can be written as

$$\Gamma_\rho^{(\rm zm)} = \frac{ig^2}{128\pi^4 p_+^2}\int d^2k_\perp [\mathcal{G}_\rho^{(x=0)} + \mathcal{G}_\rho^{(x=1)}], \tag{D11}$$

where

$$\mathcal{G}_\rho^{(x=0)} = \int_{-\epsilon}^{\epsilon} dx \int_{-L}^{L} \frac{dk_-[k_-\gamma_+ + \mathcal{M}']\gamma_\rho[k_-\gamma_+ + \mathcal{M}]}{v_1 v_2 v_2'}, \tag{D12a}$$

$$\mathcal{G}_\rho^{(x=1)} = \int_{1-\epsilon}^{1+\epsilon} dx \int_{-L}^{L} \frac{dk_-[k_-\gamma_+ + \mathcal{M}']\gamma_\rho[k_-\gamma_+ + \mathcal{M}]}{v_1 v_2 v_2'}. \tag{D12b}$$

In order to calculate these integrals, we need their asymptotical limit when $L \to \infty$ and $\epsilon \to 0$. As explained in Sec. II B 1, one should take the limit $L \to \infty$ first, while keeping ϵ finite, and then allow $\epsilon \to 0$.

We represent $\mathcal{G}_\rho^{(x=0)}$ as

$$\mathcal{G}_\rho^{(x=0)} = \int_{-\epsilon}^{\epsilon} dx \int_{-L}^{L} dk_- \Big\{\gamma_+\gamma_\rho\gamma_+ \frac{k_-^2}{v_1 v_2 v_2'} + (\mathcal{M}'\gamma_\rho\gamma_+ + \gamma_+\gamma_\rho\mathcal{M}) \frac{k_-}{v_1 v_2 v_2'} + \mathcal{M}'\gamma_\rho\mathcal{M}\frac{1}{v_1 v_2 v_2'}\Big\}.$$

For further calculations, we will make use of the formulas

$$\frac{k_-^n}{v_1 v_2 v_2'} = \frac{D_n(x)}{v_1} + \frac{E_n(x)}{v_2} + \frac{F_n(x)}{v_2'}, \qquad n = 0, 1, 2, \tag{D13}$$

where v_1, v_2, and v_2' are defined by Eqs. (D4), and the functions $D_n(x)$, $E_n(x)$, and $F_n(x)$ are

$$D_0(x) = \frac{x^2}{t_1 t_1'}, \qquad E_0(x) = \frac{x-1}{t_1 t_2}, \qquad F_0(x) = -\frac{x-1}{t_1' t_2},$$
$$D_1(x) = \frac{ax}{t_1 t_1'}, \qquad E_1(x) = \frac{b + (x-1)p_-}{t_1 t_2},$$
$$F_1(x) = -\frac{b' + (x-1)p_-'}{t_1' t_2}, \qquad D_2(x) = \frac{a^2}{t_1 t_1'},$$
$$E_2(x) = \frac{[b + (x-1)p_-]^2}{(x-1)t_1 t_2},$$
$$F_2(x) = -\frac{[b' + (x-1)p_-']^2}{(x-1)t_1' t_2}, \tag{D14}$$

with

$$t_1 = (x-1)(xp_- - a) + bx,$$
$$t_1' = (x-1)(xp_-' - a) + b'x,$$
$$t_2 = b - b' + (p_- - p_-')(x-1).$$

The values of a, b, and b' are defined by Eqs. (D2).

After the transformation (D13), the problem of finding $\mathcal{G}_\rho^{(x=0)}$ reduces to the calculation of integrals of the following three types:

$$\int_{-\epsilon}^{\epsilon} dx f(x) \int_{-L}^{L} \frac{dk_-}{v_1}, \qquad \int_{-\epsilon}^{\epsilon} dx f(x) \int_{-L}^{L} \frac{dk_-}{v_2}, \qquad \int_{-\epsilon}^{\epsilon} dx f(x) \int_{-L}^{L} \frac{dk_-}{v_2'}, \tag{D15}$$

with various functions $f(x)$, being either $D_n(x)$, $E_n(x)$, and $F_n(x)$, or their products with $\mathcal{M}$ and $\mathcal{M}'$. It is easy to see that the latter two integrals in Eqs. (D15) always give zero in the limit $\epsilon \to 0$, while the first one is of the type of the integral (E4) from Appendix E. Using the formula (E4) and taking into account that $D_2(0) = 1$, we get

$$\mathcal{G}_\rho^{(x=0)} = \gamma_+\gamma_\rho\gamma_+ \int_{-\epsilon}^{\epsilon} dx D_2(x) \int_{-L}^{L} \frac{dk_-}{v_1} = -\gamma_+\gamma_\rho\gamma_+\Big[\pi^2 + 2\pi i\Big(\log\frac{L}{a} - \log\frac{1}{\epsilon}\Big)\Big]. \tag{D16}$$

The calculation of $\mathcal{G}_\rho^{(x=1)}$ is similar, but the algebra is more lengthy. Changing the variable $x \to x - 1$, we have

$$\mathcal{G}_\rho^{(x=1)} = \int_{-\epsilon}^{\epsilon} dx \int_{-L}^{L} dk_- \Big\{\gamma_+\gamma_\rho\gamma_+ \frac{k_-^2}{u_1 u_2 u_2'} + (\mathcal{M}_1'\gamma_\rho\gamma_+ + \gamma_+\gamma_\rho\mathcal{M}_1) \frac{k_-}{u_1 u_2 u_2'} + \mathcal{M}_1'\gamma_\rho\mathcal{M}_1\frac{1}{u_1 u_2 u_2'}\Big\},$$

where

$$u_1 = (x+1)k_- - a + i0,$$
$$u_2 = xk_- - b - xp_- + i0, \tag{D17}$$
$$u_2' = xk_- - b' - xp_-' + i0,$$

$$\mathcal{M}_1 = xp_+\gamma_- - p_-\gamma_+ - 2\mathbf{k}_\perp\cdot\boldsymbol{\gamma}_\perp - 2m,$$
$$\mathcal{M}_1' = xp_+\gamma_- - p_-'\gamma_+ - 2(\mathbf{k}_\perp - \mathbf{q}_\perp)\cdot\boldsymbol{\gamma}_\perp - 2m. \tag{D18}$$

We have now, instead of Eq. (D13):

$$\frac{k_-^n}{u_1 u_2 u_2'} = \frac{D_n(x+1)}{u_1} + \frac{E_n(x+1)}{u_2} + \frac{F_n(x+1)}{u_2'}, \qquad n = 0, 1, 2. \tag{D19}$$

Again, we encounter integrals of the types (D15), v's being changed by u's. The terms with u_2 and u_2' in the denominators contribute only, while those with u_1 disappear in the limit $\epsilon \to 0$, after the integration over dx. Using the formulas (E4) and (E5) from Appendix E, we obtain after some transformations

$$\mathcal{G}_\rho^{(x=1)} = \gamma_+\gamma_\rho\gamma_+\Big\{\pi^2 + 2\pi i\Big(\log\frac{L}{a} - \log\frac{1}{\epsilon}\Big) + 2\pi i H_1(\mathbf{k}_\perp)\Big\} + 2\pi i p_+[\mathcal{M}_{10}'\gamma_\rho\gamma_+ + \gamma_+\gamma_\rho\mathcal{M}_{10}]H_2(\mathbf{k}_\perp), \tag{D20}$$

where

$$\mathcal{M}_{10} = -p_-\gamma_+ - 2\mathbf{k}_\perp \cdot \boldsymbol{\gamma}_\perp - 2m,$$
$$\mathcal{M}'_{10} = -p'_-\gamma_+ - 2(\mathbf{k}_\perp - \mathbf{q}_\perp) \cdot \boldsymbol{\gamma}_\perp - 2m,$$
$$H_1(\mathbf{k}_\perp) = \frac{p_- - p'_-}{b - b'} + \log\frac{a}{b} + \frac{(a-b')(b-b') + bp'_- - b'p_-}{(b-b')^2} \log\frac{b}{b'},$$
$$H_2(\mathbf{k}_\perp) = \frac{1}{p_+(b-b')} \log\frac{b}{b'}.$$

In order to find the form factors $\mathcal{F}^{(\mathrm{zm})}$ from the vertex $\Gamma_\rho^{(\mathrm{zm})}$, it is convenient to cast the latter in an explicitly covariant form. For this purpose we introduce the four-vectors

$$r \equiv (r_-, r_+, \mathbf{r}_\perp) = (p_-, 0, -\mathbf{k}_\perp),$$
$$r' \equiv (r'_-, r'_+, \mathbf{r}'_\perp) = (p'_-, 0, \mathbf{q}_\perp - \mathbf{k}_\perp).$$

Then, taking the sum of Eqs. (D16) and (D20), substituting it into Eq. (D11), and changing everywhere $\gamma_+ \to \not\omega$, $p_+ \to \omega \cdot p$, we arrive at the desired result:

$$\Gamma_\rho^{(\mathrm{zm})} = -\frac{g^2}{32\pi^3} \int d^2k_\perp \left\{ \frac{\not\omega \omega_\rho}{(\omega \cdot p)^2} H_1(\mathbf{k}_\perp) - \left[(\not r' + m)\gamma_\rho \frac{\not\omega}{\omega \cdot p} + \frac{\not\omega}{\omega \cdot p} \gamma_\rho (\not r + m) \right] H_2(\mathbf{k}_\perp) \right\}. \tag{D21}$$

To find the form factors, one should substitute $\Gamma_\rho^{(\mathrm{zm})}$ into Eq. (57), instead of Γ_ρ, then find c_{1-5} by means of Eqs. (58), and finally revert the system of linear equations (59) taken for $\alpha = 0$. We give here the result:

$$F_1^{(\mathrm{zm})} = F_2^{(\mathrm{zm})} = 0, \qquad B_i^{(\mathrm{zm})} = -\frac{g^2}{32\pi^3} \int d^2k_\perp b_i(\mathbf{k}_\perp),$$

where

$$b_1(\mathbf{k}_\perp) = H_2(\mathbf{k}_\perp), \qquad b_2(\mathbf{k}_\perp) = -2H_2(\mathbf{k}_\perp),$$
$$b_3(\mathbf{k}_\perp) = \frac{1}{m^2}[H_1(\mathbf{k}_\perp) - 2(\mathbf{k}_\perp \cdot \mathbf{q}_\perp + m^2)H_2(\mathbf{k}_\perp)].$$

It is convenient to use the following representations:

$$H_1(\mathbf{k}_\perp) = \int_0^1 dz \left[\frac{zp_- + (1-z)p'_- + a - b'}{bz + b'(1-z)} + \frac{a-b}{az + b(1-z)} \right],$$
$$H_2(\mathbf{k}_\perp) = \frac{1}{p_+} \int_0^1 \frac{dz}{bz + b'(1-z)},$$

which can be checked by direct integration. Calculating first the integrals over $d^2k_\perp$ and then over dz, we find the zero-mode contribution to the form factors, Eqs. (75).

APPENDIX E: CALCULATION OF THE ZERO-MODE INTEGRALS

Finding the zero-mode contribution to the self-energy and EMV requires calculation of the asymptotic value of the integral

$$I_1 = \int_{-\epsilon}^{\epsilon} dx \int_{-L}^{L} \frac{dk_-}{xk_- - b - xh + i0} \tag{E1}$$

at $L \to \infty$ and $\epsilon \to 0$ (b and h are considered as finite quantities independent both of k_- and x). As we shall see below, the real part of I_1 is finite in this limit, so that

$$\begin{aligned} \mathrm{Re}\, I_1 &= \mathrm{Re} \int_{-\epsilon}^{\epsilon} dx \int_{-\infty}^{+\infty} \frac{dk_-}{xk_- - b - xh + i0} \\ &= \mathrm{Im}\left[\lim_{\lambda\to 0} \int_{-\epsilon}^{\epsilon} dx \int_{-\infty}^{+\infty} dk_- \int_{\lambda}^{+\infty} dy e^{i(xk_- - b - xh + i0)y} \right] \\ &= 2\pi\, \mathrm{Im}\left[\lim_{\lambda\to 0} \int_{\lambda}^{+\infty} dy e^{-i(b - i0)y} \int_{-\epsilon}^{\epsilon} dx e^{-ihxy} \delta(xy) \right] \\ &= -2\pi \int_0^{+\infty} dy \frac{\sin by}{y} = -\pi^2 \,\mathrm{sgn}(b). \end{aligned}$$

The imaginary part of I_1 is divergent in L and ϵ, and we have to retain finite values of the cutoffs:

$$\mathrm{Im}\, I_1 = -\pi \int_{-\epsilon}^{\epsilon} dx \int_{-L}^{L} dk_- \delta(xk_- - b - xh).$$

Using the identity $\delta(z) = \delta(-z)$, we can easily see that $\mathrm{Im} I_1$ does not change under the transformation $b \to -b$. It is thus legitimate to substitute b by $|b|$. Calculating the integral by means of the δ-function, we get

$$\begin{aligned} \mathrm{Im}\, I_1 &= -\pi\left(\int_{-\epsilon}^{-|b|/(L+h)} \frac{dx}{|x|} + \int_{|b|/(L-h)}^{\epsilon} \frac{dx}{x} \right) \\ &= -\pi\left(\log\frac{L^2 - h^2}{b^2} + 2\log\epsilon \right). \end{aligned}$$

Collecting the results together and neglecting the terms of order $(1/L)^2$ and higher, we finally obtain

$$I_1 = -\pi^2 \,\mathrm{sgn}(b) - 2\pi i\left(\log\frac{L}{|b|} - \log\frac{1}{\epsilon} \right). \tag{E2}$$

Let us now consider the integral needed for the calculation of the zero-mode contribution to the EMV:

$$I_2 = \int_{-\epsilon}^{\epsilon} \frac{dx}{x} \int_{-L}^{L} \frac{dk_-}{xk_- - b - xh + i0}, \tag{E3}$$

where the principal value prescription for the pole at $x = 0$ is implied. The real part of I_2 is found by direct integration:

$$\begin{aligned} \mathrm{Re}\, I_2 &= \int_{-\epsilon}^{\epsilon} \frac{dx}{x} \left(\mathrm{P.V.} \int_{-L}^{L} \frac{dk_-}{xk_- - b - xh} \right) \\ &= \int_{-\epsilon}^{\epsilon} \frac{dx}{x^2} \log\left| \frac{xL - b - xh}{xL + b + xh} \right| = \frac{4h}{\epsilon L} + O\left[\left(\frac{h}{\epsilon L} \right)^3 \right]. \end{aligned}$$

We have expanded the result in a series in powers of

$1/(\epsilon L)$, retaining the leading term only. Note that according to our prescription we should first tend L to infinity, while keeping ϵ finite, and then tend ϵ to zero. Under such a convention, we obtain $\mathrm{Re} I_2 = 0$. The imaginary part of I_2 reads

$$\mathrm{Im}\, I_2 = -\pi \int_{-\epsilon}^{\epsilon} \frac{dx}{x} \int_{-L}^{L} dk_- \delta(xk_- - b - xh) = -\pi \int_{-\epsilon}^{\epsilon} \frac{dx}{x^2} \int_{-xL-b-xh}^{xL-b-xh} dy \delta(y) = \frac{2\pi h}{b}.$$

Finally,

$$I_2 = \frac{2\pi i h}{b}.$$

From the results obtained above it is easy to derive the following expressions for the generalized integrals:

$$\tilde{I}_1 = \int_{-\epsilon}^{\epsilon} dx f(x) \int_{-L}^{L} \frac{dk_-}{xk_- - b - xh + i0} = -\left[\pi^2 \operatorname{sgn}(b) + 2\pi i \left(\log\frac{L}{|b|} - \log\frac{1}{\epsilon}\right)\right] f(0), \quad \text{(E4)}$$

$$\tilde{I}_2 = \int_{-\epsilon}^{\epsilon} dx \frac{f(x)}{x} \int_{-L}^{L} \frac{dk_-}{xk_- - b - xh + i0} = \frac{2\pi i h}{b} f(0) - \left[\pi^2 \operatorname{sgn}(b) + 2\pi i \left(\log\frac{L}{|b|} - \log\frac{1}{\epsilon}\right)\right] f'(0), \quad \text{(E5)}$$

where $f(x)$ is an arbitrary function supposed to be smooth and finite at $x = 0$.

[1] J. Carbonell, B. Desplanques, V. A. Karmanov, and J.-F. Mathiot, Phys. Rep. **300**, 215 (1998).
[2] S. J. Brodsky, H. C. Pauli, and S. S. Pinsky, Phys. Rep. **301**, 299 (1998).
[3] S. J. Brodsky, J. R. Hiller, and G. McCartor, Ann. Phys. (N.Y.) **305**, 266 (2003).
[4] S. J. Brodsky, V. A. Franke, J. R. Hiller, G. McCartor, S. A. Paston, and E. V. Prokhvatilov, Nucl. Phys. **B703**, 333 (2004).
[5] S. J. Brodsky, J. R. Hiller, and G. McCartor, Ann. Phys. (N.Y.) **321**, 1240 (2006).
[6] D. Bernard, Th. Cousin, V. A. Karmanov, J.-F. Mathiot, Phys. Rev. D **65**, 025016 (2001).
[7] V. A. Karmanov, J.-F. Mathiot, and A. V. Smirnov, Phys. Rev. D **69**, 045009 (2004).
[8] J.-F. Mathiot, V. A. Karmanov, and A. V. Smirnov, Nucl. Phys. B, Proc. Suppl. **161**, 160 (2006).
[9] N. E. Ligterink and B. L. G. Bakker, Phys. Rev. D **52**, 5917 (1995); **52**, 5954 (1995).
[10] N. C. J. Schoonderwoerd and B. L. G. Bakker, Phys. Rev. D **58**, 025013 (1998).
[11] J. P. B. C. de Melo and T. Frederico, Phys. Rev. C **55**, 2043 (1997); J. P. B. C. de Melo, J. H. O. Sales, T. Frederico, and P. U. Sauer, Nucl. Phys. **A631**, 574c (1998); J. P. B. C. de Melo, T. Frederico, H. W. L. Naus, and P. U. Sauer, Nucl. Phys. **A660**, 219 (1999); H. W. L. Naus, J. P. B. C. de Melo, and T. Frederico, Few-Body Syst. **24**, 99 (1998); J. P. B. C. de Melo and T. Frederico, Braz. J. Phys. **34**, 881 (2004).
[12] B. L. G. Bakker, H.-M. Choi, and Ch.-R. Ji, Phys. Rev. D **65**, 116001 (2002).
[13] B. C. Tiburzi and G. A. Miller, Phys. Rev. D **67**, 054014 (2003).
[14] F. Bissey and J.-F. Mathiot, Eur. Phys. J. C **16**, 131 (2000).
[15] W. Jaus, Phys. Rev. D **67**, 094010 (2003).
[16] B. L. G. Bakker, M. A. DeWitt, Ch.-R. Ji, and Yu. Mishchenko, Phys. Rev. D **72**, 076005 (2005).
[17] Ch.-R. Ji, B. L. G. Bakker, and H.-M. Choi, Nucl. Phys. B, Proc. Suppl. **161**, 102 (2006).
[18] J.-J. Dugne, V. A. Karmanov, and J.-F. Mathiot, Eur. Phys. J. C **22**, 105 (2001).
[19] V. A. Karmanov, Zh. Eksp. Teor. Fiz. **71**, 399 (1976) [Sov. Phys. JETP **44**, 210 (1976)].
[20] V. A. Karmanov and J.-F. Mathiot, Nucl. Phys. **A602**, 388 (1996).
[21] P. Grangé and E. Werner, Nucl. Phys. B, Proc. Suppl. **161**, 75 (2006).